Published June 20, 2016

Gut microbiota translocation to the pancreatic lymph nodes triggers NOD2 activation and contributes to T1D onset

Frederico R.C. Costa,[1] Marcela C.S. Françozo,[1] Gabriela G. de Oliveira,[1] Aline Ignacio,[4] Angela Castoldi,[4] Dario S. Zamboni,[2] Simone G. Ramos,[3] Niels O. Câmara,[4] Marcel R. de Zoete,[5,6,7] Noah W. Palm,[5] Richard A. Flavell,[5,6] João S. Silva,[1] and Daniela Carlos[1]

[1]Department of Biochemistry and Immunology, [2]Department of Molecular and Cell Biology, and [3]Department of Pathology, Ribeirão Preto Medical School, University of São Paulo, 14049-900 Ribeirão Preto, São Paulo, Brazil
[4]Department of Immunology, Institute of Biomedical Science (ICB), University of São Paulo, 05508-000 São Paulo, Brazil
[5]Department of Immunobiology, Yale University School of Medicine, The Anlyan Center, New Haven, CT 06519
[6]Howard Hughes Medical Institute, Yale University, New Haven, CT 06510
[7]Department of Infectious Diseases and Immunology, Utrecht University, 3584 CL Utrecht, the Netherlands

Type 1 diabetes (T1D) is an autoimmune disease that is triggered by both genetic and environmental factors, resulting in the destruction of pancreatic β cells. The disruption of the intestinal epithelial barrier and consequent escape of microbial products may be one of these environmental triggers. However, the immune receptors that are activated in this context remain elusive. We show here that during streptozotocin (STZ)-induced T1D, the nucleotide-binding oligomerization domain containing 2 (NOD2), but not NOD1, participates in the pathogenesis of the disease by inducing T helper 1 (Th1) and Th17 cells in the pancreatic LNs (PLNs) and pancreas. Additionally, STZ-injected wild-type (WT) diabetic mice displayed an altered gut microbiota compared with vehicle-injected WT mice, together with the translocation of bacteria to the PLNs. Interestingly, WT mice treated with broad-spectrum antibiotics (Abx) were fully protected from STZ-induced T1D, which correlated with the abrogation of bacterial translocation to the PLNs. Notably, when Abx-treated STZ-injected WT mice received the NOD2 ligand muramyl dipeptide, both hyperglycemia and the proinflammatory immune response were restored. Our results demonstrate that the recognition of bacterial products by NOD2 inside the PLNs contributes to T1D development, establishing a new putative target for intervention during the early stages of the disease.

Type 1 diabetes (T1D) is an autoimmune disease that is triggered when immunological tolerance to self-tissues fails, resulting in the autoimmune destruction of pancreatic β cells in genetically predisposed individuals. Although genetic factors play a role in susceptibility to T1D, it is possible that the increase in its prevalence is also a result of environmental factors (Gillespie et al., 2004). In this context, many experimental models have been used to study T1D, such as nonobese diabetic (NOD) mice and biobreeding rats, in which the disease develops spontaneously, and mouse models induced by chemicals, such as streptozotocin (STZ), cyclophosphamide, and alloxan (Rees and Alcolado, 2005; Yaochite et al., 2013).

Although the NOD mouse is the most widely used model to study T1D, it has some limitations that must be considered when translating its results to clinical studies. In comparison to human islets, for example, NOD mice exhibit much stronger insulitis as shown by histopathology, which, according to van Belle et al. (2011), is like looking at two different diseases. These differences could help explain why some successful treatments in the NOD mouse model failed to show the same efficacy when used in humans (Gitelman et al., 2013; Moran et al., 2013; Reed and Herold, 2015). Therefore, studying other mouse models of the disease should also be considered, especially because other rodent models have several features, such as phenotype and islet cellular infiltrates, which more closely mimic human disease than the NOD mouse (Reed and Herold, 2015). In this regard, the STZ model appears to be an interesting alternative because, in addition to resembling the disease in humans in various aspects (Like and Rossini, 1976; Leiter, 1982), it also represents an immune-mediated mouse model of the disease. In this context, it was shown that the transfer of splenocytes from STZ-injected mice causes insulin resistance and diabetes upon adoptive transfer (Paik et al., 1980; Arata et al., 2001). Accordingly, it has also been shown that athymic nude (*nu/nu*) mice are resistant to STZ-induced diabetes compared with euthymic (+/*nu*) mice (Paik et al., 1980).

Correspondence to Daniela Carlos: danicar@usp.br

Abbreviations used: Abx, antibiotics; GTT, glucose tolerance test; ITT, insulin tolerance test; MDP, muramyl dipeptide; MLN, mesenteric LN; NLR, nucleotide-binding domain and leucine-rich repeat containing receptor; NOD, non-obese diabetic mouse; NOD2, nucleotide-binding oligomerization domain containing 2; NOR, nonobese resistant mouse; PLN, pancreatic LN; STZ, streptozotocin; T1D, type 1 diabetes; Th, T helper; T reg, regulatory T.

The Rockefeller University Press $30.00
J. Exp. Med. 2016 Vol. 213 No. 7 1223–1239
www.jem.org/cgi/doi/10.1084/jem.20150744

Published June 20, 2016

In addition, anti-insulin antibodies were found in the sera of naive C57BL/6 mice, which are susceptible to STZ-induced diabetes, demonstrating another sign of an autoimmune response in this model (Elias et al., 1994).

Although there have been many studies examining the final effector mechanisms of adaptive immunity in T1D, relatively little information exists concerning the innate immune response in the development of this disease (Kim et al., 2007; Valle et al., 2013). Several lines of evidence support a role for viral infections, especially those caused by enteroviruses, as a causative agent of T1D. Members of the coxsackievirus B (CVB) species have been reported to infect human pancreatic β cells and induce the expression of proinflammatory genes, thus contributing to β cell death (Ylipaasto et al., 2012). Recently, the detection of a low-grade enteroviral infection in the islets of patients newly diagnosed with T1D has been reported (Krogvold et al., 2015), which further supports the notion that viral infections may contribute to disease progression. In mice, several virally induced mouse models of T1D have been established, such as mouse models infected with the encephalomyocarditis virus (Craighead and McLane, 1968) or CVB (Yoon et al., 1979), or the mouse model in which the host is genetically altered to express a viral antigen on their pancreatic β cells (RIP-LCMV mouse model; von Herrath et al., 1994; Coppieters et al., 2012).

The intestinal microbiota has also been considered an important component of T1D development (van Belle et al., 2011; Sorini and Falcone, 2013). However, whether it plays a protective or pathogenic role in the disease remains controversial. In this context, it has been shown that, in rodent models, diabetes is aggravated upon administration of antibiotics (Abx; Bach, 2002). Other studies, however, have shown the exact opposite (Brugman et al., 2006). In humans, subclinical immune activation (Savilahti et al., 1999; Westerholm-Ormio et al., 2003) and signs of impaired T reg subsets (Tiittanen et al., 2008) in the intestine of T1D patients were found. Additionally, it has been shown that T1D diabetic patients have alterations in the epithelial barrier of the gut, the so-called leaky gut (Vaarala et al., 2008), which also indicates a possible correlation between the gut microbiota and T1D development.

Nonetheless, the precise mechanisms by which the intestinal microbiota contribute to autoimmunity remain poorly understood. In this regard, it has been shown that microbe-associated molecular patterns derived from the microbiota activate the host innate immune system via pattern-recognition receptors, such as TLRs and nucleotide-binding domain and leucine-rich repeat containing receptors (NLRs) present in intestinal epithelial and myeloid cells (Tsuji et al., 2012). Thus, the activation of TLRs and NLRs could be implicated in the mechanisms by which bacterial translocation and further recognition trigger autoimmune diseases. The nucleotide-binding oligomerization domain containing 2 (NOD2) is an intracellular receptor that belongs to the NLR family and recognizes the bacterial component muramyl dipeptide (MDP). NOD2 has been shown to play an important role in maintaining gut homeostasis (Benjamin et al., 2013) and to induce a proinflammatory immune response by myeloid cells, thus promoting immunity against a variety of viral and bacterial pathogens (Philpott et al., 2014). However, the possible role of this receptor in recognizing translocated bacteria from the gut and triggering autoimmune diseases is still undetermined. Considering that TLR2$^{-/-}$ (Devaraj et al., 2011b), TLR4$^{-/-}$ (Devaraj et al., 2011a), and Myd88$^{-/-}$ (Bollyky et al., 2009) mice have been shown to develop STZ-induced T1D equivalently to WT mice, we aimed to evaluate the role of the NOD2 receptor in the pathogenesis of T1D using the multiple low doses (MLD-STZ) mouse model. Our data demonstrate that STZ-injected WT mice display an altered gut microbiota, accompanied by the translocation of commensal bacteria from the intestinal tract to the pancreatic LNs (PLNs) in STZ-induced diabetes. This translocation is responsible for the activation of the NOD2 receptor in myeloid cells inside the PLNs, thereby driving the differentiation of pathogenic Th1 and Th17 cells, which in turn contributes to the pathogenesis of the disease.

RESULTS

NOD2 receptor activation confers susceptibility to STZ-induced T1D development

To evaluate the role of NOD2 in the pathogenesis of T1D, C57BL/6 WT male mice were inoculated intraperitoneally with multiple low doses of STZ (MLD-STZ; 40 mg/kg) for five consecutive days. They were then assessed for mRNA expression of *Rip2*, *Nod1*, and *Nod2* in the PLNs 7 and 15 d after starting the STZ injections (Fig. 1 A). Only a small difference in *Rip2* expression was found on day 7, but we observed an increase in *Rip2*, *Nod1*, and *Nod2* mRNA expression in the PLNs on day 15 in mice injected with STZ compared with naive mice (Fig. 1, B, C, and D, respectively). Of note, no differences in mRNA expression between naive and vehicle-injected WT mice were found (unpublished data).

We also evaluated the expression of *Rip2*, *Nod1*, and *Nod2* in the NOD mouse model of T1D. Corroborating our results in the STZ model, we found an increase in *Nod1* and *Nod2* but not *Rip2* expression in the PLNs of prediabetic NOD mice (10–12 wk of age) compared with diabetes-resistant NOR (nonobese-resistant) mice (Fig. 1, E–G). To further explore whether NOD1 or NOD2 has an effect on T1D development, we used the MLD-STZ model in WT, Rip2$^{-/-}$, NOD1$^{-/-}$, and NOD2$^{-/-}$ mice, and disease incidence was monitored. Interestingly, Rip2$^{-/-}$ and NOD1$^{-/-}$ mice were as susceptible to STZ-induced diabetes as WT mice, presenting a robust increase in their blood glucose levels (Fig. 1 H), and became diabetic similarly to WT mice (Fig. 1, I and J, respectively). Surprisingly, the majority of NOD2$^{-/-}$ mice did not develop hyperglycemia after the STZ injections (Fig. 1 H) and were protected from STZ-induced diabetes ($P = 0.0008$; Fig. 1 K). Blood glucose levels were analyzed for up to 1 mo after the STZ injections in the NOD2$^{-/-}$ mice cohort, and whereas STZ-injected WT mice

Published June 20, 2016

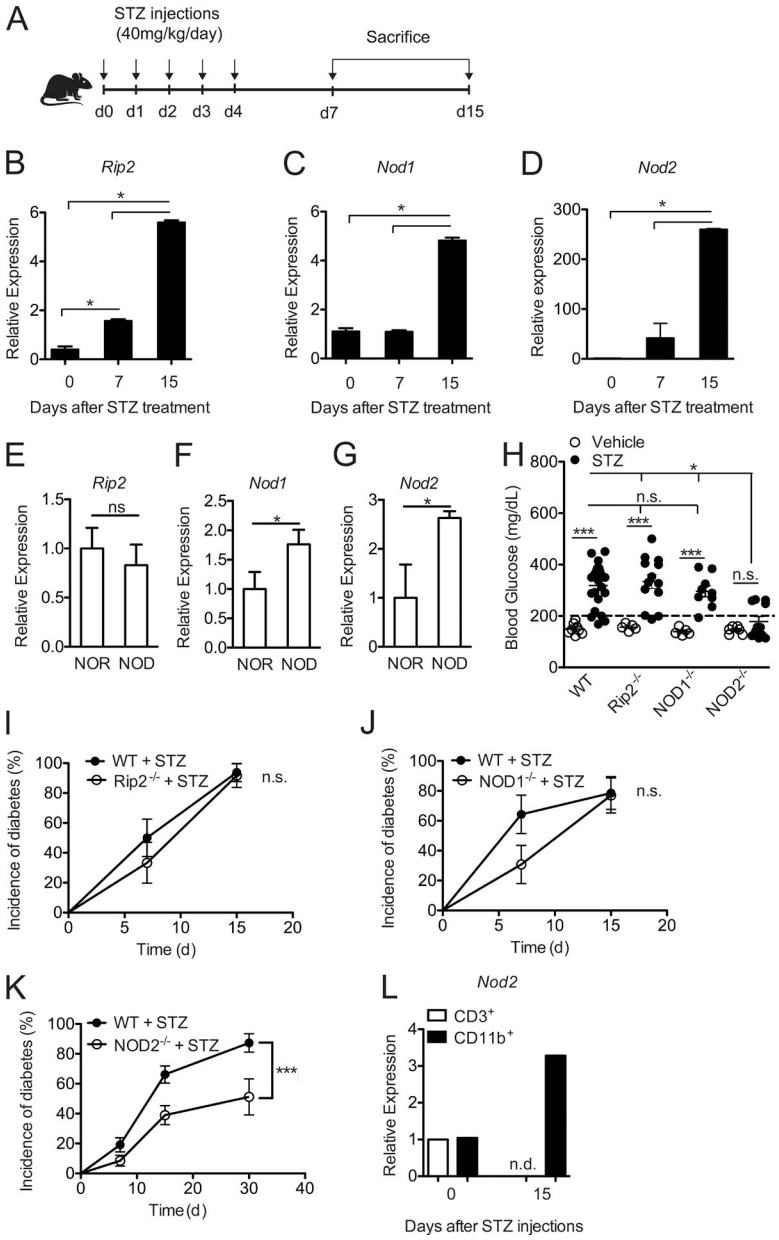

Figure 1. **The NOD2 receptor contributes to T1D pathogenesis.** WT and NOD2$^{-/-}$ mice were injected with STZ or vehicle solution (nondiabetic) for five consecutive days (40 mg/kg/d). The PLNs were recovered at 7 and 15 d after the start of STZ injections (A) for the quantification of the relative mRNA expression of *Rip2* (B), *Nod1* (C), and *Nod2* (D) by RT-PCR. NOD mice and NOR mice (10–12 wk of age) were sacrificed to collect the PLNs for the analysis of *Rip2* (E), *Nod1* (F), and *Nod2* (G) gene expression by RT-PCR. C57BL/6 mice lacking Rip2 (I), NOD1 (J), and NOD2 (K) were also analyzed for blood glucose levels 15 d after the STZ injections (H) and diabetes incidence. CD3$^+$ lymphoid or CD11b$^+$ myeloid cells from the PLNs were isolated by FACS from WT diabetic or nondiabetic mice 15 d after the STZ injections and were assessed for the mRNA relative expression of *Nod2* by RT-PCR (L). The results are expressed as the mean ± SEM (n = 3–10 mice per group). The results are representative of at least two independent experiments or a compilation of two to ten different experiments (H-K). *, P ≤ 0.05 was considered statistically significant; ***, P≤ 0.001; n.s. = not significant; n.d. = not detected.

reached ∼90% disease incidence, only half of the STZ-injected NOD2$^{-/-}$ mice developed the disease after the STZ injections (Fig. 1 K). To investigate if NOD2 is important in the myeloid or lymphoid compartment, myeloid CD11b$^+$ and lymphoid CD3$^+$ cells were isolated from the PLNs of diabetic mice and assessed for *Nod2* mRNA expression by RT-PCR. We found that *Nod2* is up-regulated 15 d after the STZ injections in myeloid, but not lymphoid, cells (Fig. 1 L), indicating that this receptor possibly mediates its effects in the myeloid compartment. These data indicate that NOD2, in a Rip2-independent pathway, has an important role in STZ-induced T1D pathogenesis.

To confirm our findings, we analyzed clinical parameters, such as blood glucose kinetics and body weight. In fact, WT mice had increased blood glucose levels on day 10 and reached a peak on day 15 after the STZ injections, whereas most of the NOD2$^{-/-}$ mice remained euglycemic throughout the same period (Fig. 2 A). Additionally, NOD2$^{-/-}$ mice did not lose body weight compared with WT mice (Fig. 2 B). To assess whether the hyperglycemia caused by the STZ injections is a consequence of insufficient insulin production or insulin resistance, both glucose tolerance tests (GTT) and insulin tolerance tests (ITTs) were performed. As expected, STZ-injected WT mice exhibited impaired glucose tolerance, whereas NOD2$^{-/-}$ mice were able to restore their blood glucose levels back to normal (Fig. 2 C). Interestingly, when STZ-injected WT mice were provided with insulin during the ITT test, they were able to respond and de-

Published June 20, 2016

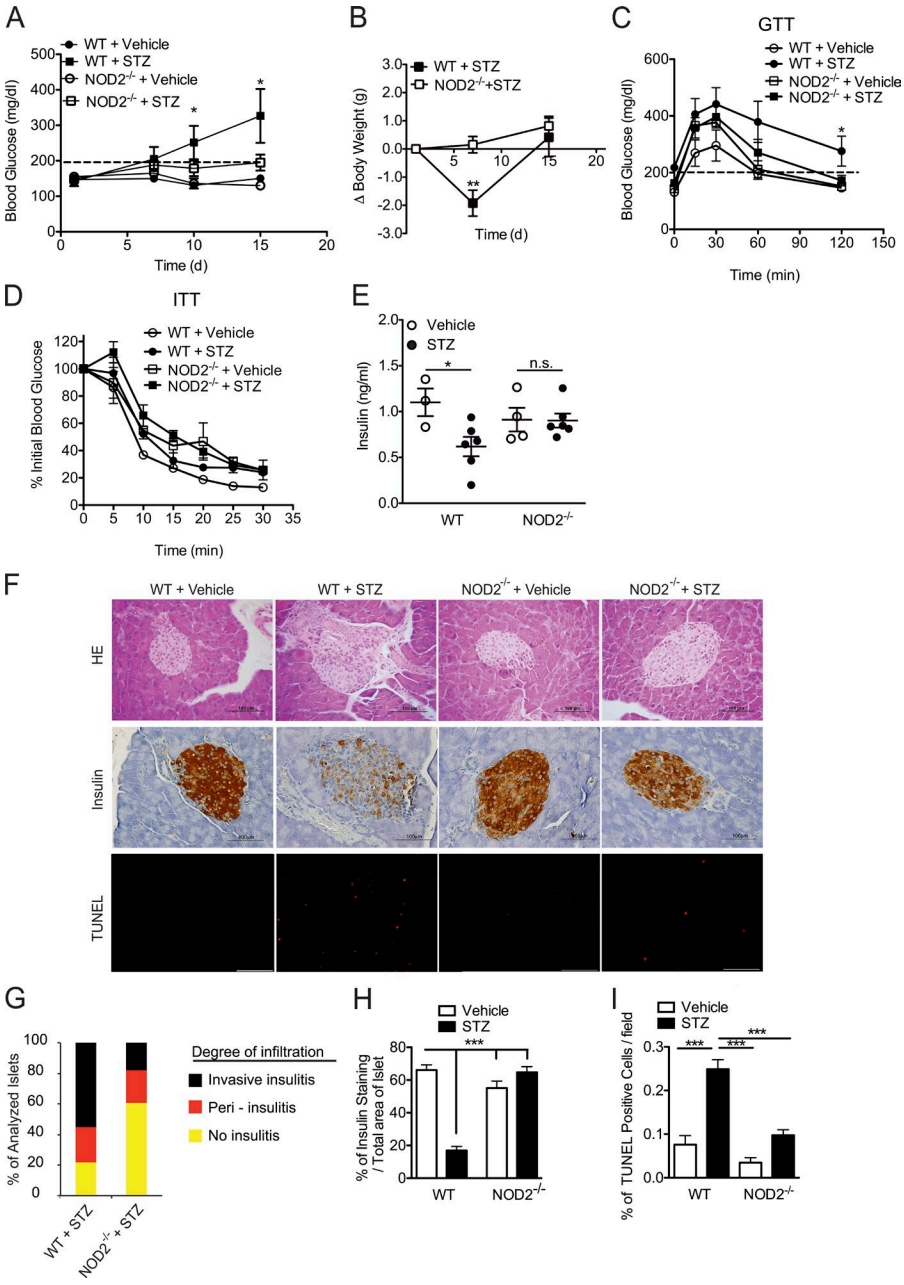

Figure 2. **NOD2 is required for the inflammatory infiltrate inside the pancreatic islets in T1D.** WT and NOD2$^{-/-}$ mice were injected with STZ or vehicle solution (nondiabetic) for five consecutive days (40 mg/kg/d). The mice were analyzed for blood glucose levels at days 1, 7, 10, and 15 (A) and body weight was monitored at days 1, 7, and 15 after beginning the STZ injections (B). These mice were then sacrificed on day 15, and the serum was recovered for insulin quantification by ELISA (E). On day 15, both GTT (C) and ITT (D) were performed on WT or NOD2$^{-/-}$ mice injected with STZ or vehicle solution. The inflammatory infiltrate within the pancreatic islets (insulitis; F, top), insulitis score (G), insulin expression (F, middle), and β cell death (F, bottom) of WT and NOD2$^{-/-}$ mice were assessed by H&E staining (40×), immunohistochemistry, or TUNEL assay (20×), respectively. A quantitative analysis of insulin expression by immunohistochemistry (H) and β cell death by TUNEL assay (I) of WT and NOD2$^{-/-}$ mice was performed using ImageJ software (National Institutes of Health). The results are representative of two independent experiments. The results are expressed as the mean ± SD (A) or the mean ± SEM (B–E and H–I; n = 4–6 mice per group). *, $P \leq 0.05$; ***, $P \leq 0.001$; n.s. = not significant.

crease their blood glucose levels similarly to vehicle-injected WT mice (Fig. 2 D), thus indicating that the hyperglycemia observed after the STZ injections is a consequence of the absence of insulin production and not of insulin resistance. Consistent with the observed resistance of NOD2$^{-/-}$ mice to STZ-induced diabetes, STZ-injected WT mice presented lower levels of insulin in the serum, whereas STZ-injected NOD2$^{-/-}$ mice had normal levels (Fig. 2 E).

To test whether the resistance observed in NOD2$^{-/-}$ mice to STZ-induced T1D could be attributed to a reduced proinflammatory response within the pancreatic islets, WT and NOD2$^{-/-}$ mice were injected with STZ, and both inflammatory and histological parameters were assessed. Histological analysis showed that STZ-injected NOD2$^{-/-}$ mice exhibited a milder inflammatory infiltrate (insulitis) with less invasive insulitis in the pancreatic islets (Fig. 2, F, top, and G) Consistent with these results, NOD2$^{-/-}$ mice exhibited increased staining for insulin relative to WT mice in the pancreatic islets after the STZ injections (Fig. 2, F, middle, and H). We also performed TUNEL staining to determine the extent of β cell death and, in agreement with the insulitis score and insulin staining, STZ-injected NOD2$^{-/-}$ mice showed lower TUNEL staining compared with STZ-injected WT mice (Fig. 2, F, bottom, and I). Collectively, these data sug-

Published June 20, 2016

gest that NOD2 activation leads to the destruction of insulin-producing β cells in the pancreatic islets, resulting in the onset of STZ-induced diabetes.

NOD2 receptor activation in DCs and macrophages induces a proinflammatory immune response in STZ-induced T1D

NOD2 has been shown to be highly expressed by DCs (Tada et al., 2005) and macrophages (Caetano et al., 2011). Because we found that NOD2 mediates its effects through the myeloid compartment (Fig. 1 L), we next assessed whether NOD2 deficiency suppressed the induction of a proinflammatory immune response by myeloid cells, thus contributing to STZ-induced diabetes resistance. In fact, in vitro experiments with bone marrow–derived DCs from NOD2$^{-/-}$ mice stimulated with the NOD2 ligand, MDP, and LPS showed a lower production of cytokines related to Th17 and Th1 cell polarization, such as IL-1β, IL-6, IL-23, and IL-12p40, compared with DCs from WT mice (Fig. 3, A–D, respectively). To further confirm the importance of NOD2 in driving Th1 and Th17 differentiation, bone marrow–derived DCs from WT or NOD2$^{-/-}$ mice were co-cultured with naive CD4$^+$ T cells in the presence of MDP for 5 d. As expected, MDP induced the differentiation of Th1 (Fig. 3, E and G) and Th17 cells (Fig. 3, F and H) in vitro only in the presence of bone marrow–derived DCs from WT, but not from NOD2$^{-/-}$, mice. These results suggest that NOD2 activation in DCs is implicated in the production of proinflammatory cytokines required for the generation and expansion of Th1 and Th17 cells in vitro.

To assess the role of the NOD2 receptor in triggering a pathogenic immune response in vivo, NOD2$^{-/-}$ and WT mice were injected with STZ and, 15 d later, the production of proinflammatory cytokines, such as IL-6 and IL-12, was assessed in the PLNs by flow cytometry (Fig. 4, A–D). DCs (Fig. 4, A and B) and macrophages (Fig. 4, C and D) from STZ-injected NOD2$^{-/-}$ mice failed to induce the production of IL-6 and IL-12 in the PLNs compared with STZ-injected WT mice.

Because DCs and macrophages from STZ-injected NOD2$^{-/-}$ mice failed to promote a proinflammatory immune response in the PLNs, we then assessed whether these cells were actually inducing a tolerogenic immune response, thus corroborating the resistance observed in NOD2$^{-/-}$ mice. Surprisingly, macrophages from STZ-injected NOD2$^{-/-}$ mice presented an increased expression of CD206, a known marker of an antiinflammatory M2 phenotype (Fig. 4 E). On the other hand, DCs from STZ-injected NOD2$^{-/-}$ mice had a robust increase in the expression of CD11b (CD11c$^+$CD11b$^+$ cells) inside the PLNs (Fig. 4 F) and pancreas (Fig. 4 G), which has previously been associated with a tolerogenic DC phenotype in a mouse model of T1D (Kriegel et al., 2012). To confirm this tolerogenic phenotype, the production of IL-10 inside the CD11b$^+$ or CD11b$^-$ compartments (gated on CD11c$^+$ cells) was analyzed in the pancreatic tissue of both STZ-injected WT and NOD2$^{-/-}$ mice. As demonstrated in Fig. 4 H, the CD11b$^+$ compartment accounts for most of the IL-10 production in

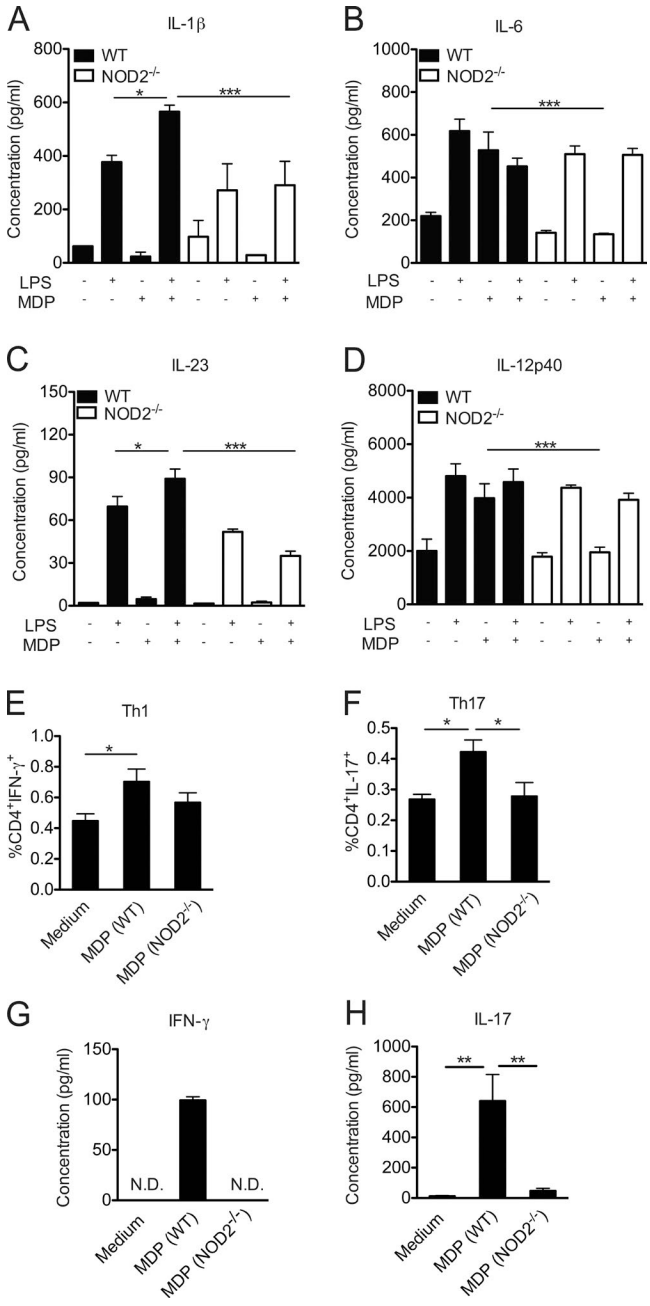

Figure 3. **NOD2 activation triggers a proinflammatory response in vitro.** Bone marrow–derived DCs from WT or NOD2$^{-/-}$ mice were stimulated with LPS alone (200 ng/ml) for 24 h in the presence or absence of MDP (10 µg/ml). The levels of IL-1β (A), IL-6 (B), IL-23 (C), and IL-12p40 (D) were measured in the supernatant by ELISA. Alternatively, bone marrow–derived DCs from WT or NOD2$^{-/-}$ mice were co-cultured with naive CD4$^+$ T cells in the presence of MDP (10 µg/ml) for 5 d and were then assessed for the presence of CD4$^+$ IFN-γ$^+$ (Th1; E) and CD4$^+$IL-17$^+$ (Th17; F) cells by flow cytometry. The concentrations of IFN-γ (G) and IL-17 (H) were measured in the supernatant by ELISA. The results are expressed as the mean ± SEM. At least four technical replicates per group were used in each in vitro experiment. *, P ≤ 0.05; **, P ≤ 0.01; ***, P ≤ 0.001.

Published June 20, 2016

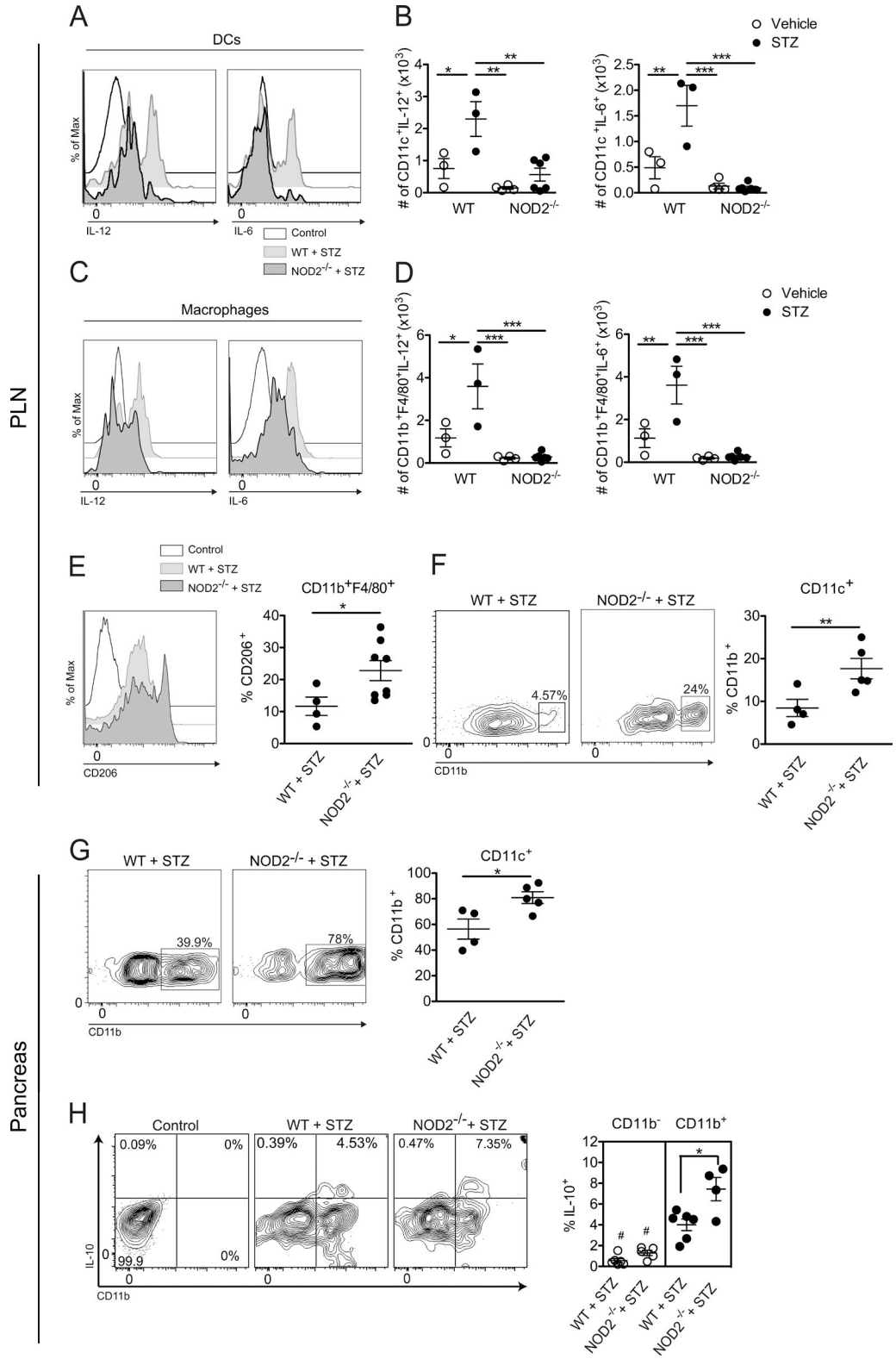

Figure 4. **NOD2 activation triggers a proinflammatory immune response by myeloid cells in vivo.** Cells from the PLNs (A–F) and pancreas (G and H) of WT or NOD2$^{-/-}$ mice were harvested 15 d after vehicle or STZ administration. The frequency and absolute numbers of IL-6– and IL-12–producing DCs (CD11c$^+$; A and B) and macrophages (Mϕs; CD11b$^+$F4/80$^+$; C and D) were assessed by flow cytometry. Next, the frequency of CD206$^+$ cells gated on CD11b$^+$F4/80$^+$ (M2 macrophages) was assessed by flow cytometry (E). Additionally, the expressions of CD11b in DCs from the PLNs (F) and pancreas (G),

Published June 20, 2016

both WT and NOD2$^{-/-}$ mice injected with STZ, thus corroborating a tolerogenic role of these double-positive DCs. Interestingly, we also observed a small, yet statistically significant, increase in the IL-10 production from CD11c^{+}CD11b^{+} DCs from STZ-injected NOD2$^{-/-}$ mice compared with WT mice (Fig. 4 H, closed circles). Overall, these results suggest that the activation of the NOD2 receptor plays an important role in inducing a proinflammatory immune response by myeloid cells in the PLNs, thus contributing to STZ-induced T1D.

NOD2 receptor activation is involved in the generation of Th1 and Th17 cells in vivo in STZ-induced T1D

Because DCs and macrophages from mice lacking NOD2 produce less cytokines related to the generation of Th1 and Th17 cells in vitro and in vivo, we next investigated whether NOD2 deficiency interferes with Th1 and Th17 cell populations in vivo. As expected, STZ-injected NOD2$^{-/-}$ mice had lower frequencies and absolute numbers not only of Th1 and Th17 cells but also of Tc1 and Tc17 cells compared with STZ-injected WT diabetic mice in the PLNs (Fig. 5, A–C). The decreased numbers of Th1 and Th17 cells in the PLNs correlated with lower levels of Th1 and Th17 cells in the pancreatic tissue (Fig. 5, E and F). These findings confirmed that NOD2 activation in the PLNs leads to the generation of Th1 and Th17 cells during STZ-induced T1D development. Interestingly, STZ-injected Rip2$^{-/-}$ mice were able to mount a Th1 and Th17 cell immune response (Fig. 5 D) similar to that seen in STZ-injected WT mice (Fig. 5, A–C), indicating that NOD2 is possibly recruiting another adaptor molecule besides Rip2 to induce the differentiation of Th1 and Th17 cells in vivo during STZ-induced diabetes.

In addition, we observed that the absolute numbers of regulatory T (T reg) cells were elevated in the PLNs of STZ-injected NOD2$^{-/-}$ mice compared with STZ-injected WT mice (Fig. 5 G). Consistent with these results, the Foxp3/RORγt ratio was also found to be increased in the PLNs of STZ-injected NOD2$^{-/-}$ mice compared with STZ-injected WT mice (Fig. 5 I). Additionally, higher IL-10 production (Fig. 5 H) and consequential increases in the IL-10/IL-17 ratio (Fig. 5 J) in the pancreatic tissue were also observed in NOD2$^{-/-}$ mice after STZ injections. These data suggest that NOD2 receptor activation skews the immune response toward a Th1 and Th17 profile over T reg cells, thus favoring the onset of STZ-induced T1D.

Gut microbiota translocation to the PLNs is implicated in T1D development

Several studies have demonstrated a possible interaction between altered intestinal microbiota and T1D (Secondulfo et al., 2004; Bosi et al., 2006; Brugman et al., 2006; Vaarala et al., 2008; Brown et al., 2011; Sorini and Falcone, 2013). However, it is still unclear how the intestinal microbiota can affect autoimmune processes at sites distal from the intestine, such as the pancreatic islets (Sorini and Falcone, 2013). Because NOD2 was found to be up-regulated in the PLNs of diabetic mice (Fig. 1, D and G), we hypothesized that the activation of this receptor could be caused by bacterial translocation from the gut to the PLNs. We detected bacteria inside the PLNs of STZ-injected WT mice by CFU and 16S PCR analysis (Fig. 6, A and B, respectively). Interestingly, we also found a sixfold increase in 16S rRNA expression in the PLNs of NOD mice compared with NOR mice (Fig. 6 B). Thus, to further assess the contribution of the gut microbiota to activating the NOD2 receptor inside the PLNs, WT mice were provided daily doses of a cocktail of four Abx (metronidazole, vancomycin, ampicillin, and neomycin) for 2 wk before the STZ injections. Alternatively, WT mice were given MDP in the drinking water during the antibiotic treatment and STZ injections (Fig. 6 C). Interestingly, we detected the presence of bacteria not only in the PLNs but also inside the mesenteric LNs (MLNs; Fig. 6 D). Surprisingly, antibiotic treatment prevented bacterial translocation to the PLNs but not to the MLNs (Fig. 6 D).

It has been demonstrated that dysbiosis is intimately related to bacterial translocation (O'Brien et al., 2014; Dinh et al., 2015; Earley et al., 2015). Therefore, to investigate whether the bacterial translocation to the MLNs and PLNs observed in STZ-injected WT mice is related to differences in the gut microbial composition, we analyzed the composition of the gut microbiota of diabetic mice by 16S rRNA gene sequencing. Interestingly, several differences were found between groups at the genera level (Fig. 6 E). More specifically, the *Bacteroides* (phylum Bacteroidetes, family Bacteroidaceae), *Oscillospira* (phylum Firmicutes, family Ruminococcaceae), *Sutterella* (phylum Proteobacteria, family Alcaligenaceae), and *Bifidobacterium* (phylum Actinobacteria, family Bifidobacteriaceae) genera increased only in STZ-injected WT mice but not in the other groups. Notably, the *Oscillospira* genus has been reported as an important gut microbe that disrupts the gut epithelial barrier and contributes to bacterial translocation in a mouse model of obesity (Lam et al., 2012).

We also analyzed the taxonomic abundance using the linear discriminant analysis effect size (Segata et al., 2011; Palm et al., 2014) to determine which bacterial taxa were significantly increased in the gut microbiota of all groups. Using this analysis, we found that the genus *Bacte-*

along with the IL-10 production by CD11b^{+} or CD11b^{-} cells (gated on CD11c^{+} cells) in the pancreatic tissue (H), were also analyzed by flow cytometry. Doublets exclusion and a pregate excluding lymphocytes based on FSC/SSC were performed. Data are representative of at least two independent experiments. The results are expressed as the mean ± SEM (n = four to six mice per group). $^{\#}$, $P \leq 0.05$ compared with CD11b^{+} compartment; *, $P \leq 0.05$; **, $P \leq 0.01$; ***, $P \leq 0.001$.

Published June 20, 2016

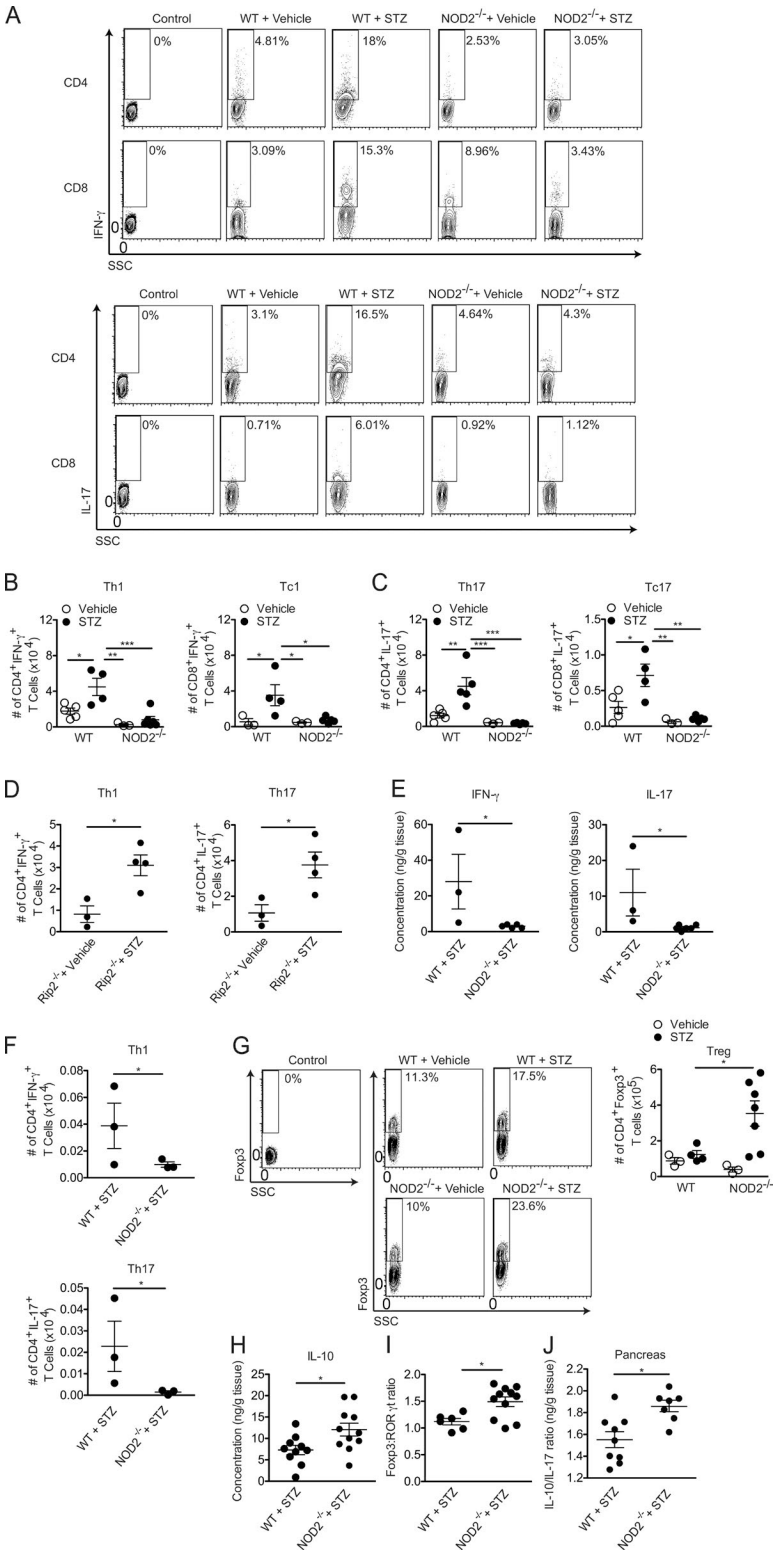

Figure 5. **The NOD2 receptor is involved in the generation of Th1 and Th17 cells in vivo.** Cells from the PLNs (A, B, C, D, G, and I) or pancreas (F) of WT, Rip2$^{-/-}$, or NOD2$^{-/-}$ mice were harvested 15 d after vehicle or STZ administration. The frequency (A and G) and absolute numbers (B–D, F, G, and I) of CD4$^+$IFN-γ$^+$ (Th1), CD8$^+$IFN-γ$^+$ (Tc1), CD4$^+$IL-17$^+$(Th17), CD8$^+$IL-17$^+$(Tc17), and CD4$^+$Foxp3$^+$(T reg) cells and the Foxp3/RORγt cell ratio were assessed by flow cytometry. The gate was set on CD3$^+$ T cells. Alternatively, the production of IFN-γ and IL-17 (E), IL-10 alone (H), or the IL-10/IL-17 ratio (J) was measured in the pancreatic tissue by ELISA 15 d after the STZ injections. Data are representative of at least two independent experiments. The results are expressed as the mean ± SEM (n = 4–6 mice per group). *, P ≤ 0.05; **, P ≤ 0.01; ***, P ≤ 0.001.

roides, the family Bacteroidaceae, and the phylum Proteobacteria were significantly increased in STZ-injected WT mice compared with vehicle-injected WT mice (Fig. 6 F). Interestingly, the genera *Akkermansia* (phylum Verrucomicrobia, family Verrucomicrobiaceae) and *Parabacteroides* (phylum Bacteroidetes, family Porphyromonadaceae) were enriched in Abx-treated STZ-injected WT mice compared with STZ-injected WT mice. In contrast, the

Published June 20, 2016

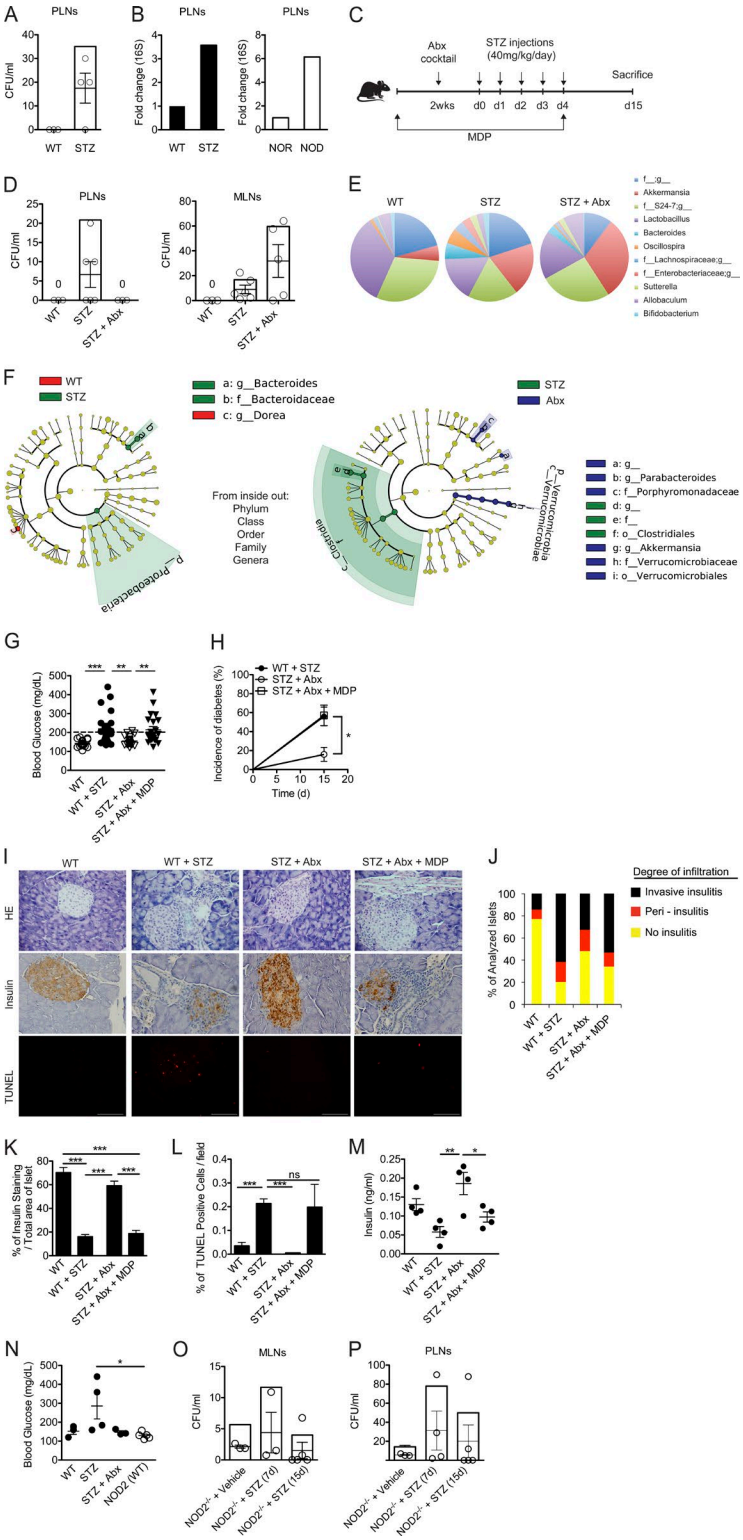

Figure 6. **Gut microbiota translocation to the PLNs triggers NOD2 activation.** Vehicle or STZ-injected WT mice were sacrificed, and PLNs were collected for the analysis of bacterial translocation by counting CFU (A) or 16S PCR (B). NOD and NOR mice (10–12 wk of age) were also sacrificed for the analysis of 16S expression in the PLNs by PCR (B). Alternatively, WT (C57BL/6) mice were administered daily doses of a cocktail of Abx for 2 wk before the injections with STZ (C). During the Abx and STZ administration, mice were supplemented or not supplemented with MDP in the drinking water at a fixed concentration of 1 µM. The PLNs and MLNs (D) of WT mice were recovered 15 d after vehicle or STZ administration. The samples were then cultured on BHI agar medium for 48 h at 37°C, and CFU was assessed. The relative abundance of fecal bacterial genera (E) of vehicle-injected, STZ-injected, and Abx-treated STZ-injected WT mice was evaluated by 16S rRNA gene sequencing (F). A taxonomic cladogram comprising all detected taxa. Bacterial taxa that were significantly different among all pairwise comparisons were used as inputs for the Linear Discriminant Analysis Effect Size software. The rings of the cladogram stand for phylum (innermost), class, order, family, and genus (outermost), respectively. Enlarged colored circles are the differentially abundant taxa identified to be metagenomic biomarkers. Mice treated as in C were analyzed for blood glucose levels (G), diabetes incidence (H), the inflammatory infiltrate (I [top] and J), insulin production within the pancreatic tissue (I [middle] and K) and the extent of β cell death (I [bottom] and L) by H&E, immunohistochemistry, and TUNEL assay, respectively. Insulin levels in the serum were also quantified (M). NOD2$^{-/-}$ mice treated with Abx were given fecal samples from C57BL/6 WT mice (NOD2(WT)) and were then injected with STZ for the assessment of the blood glucose levels 15 d later (N). The MLNs (O) and PLNs (P) of NOD2$^{-/-}$ mice injected with STZ or vehicle solution were recovered 7 or 15 d after the injections and were assessed for the presence of bacteria by CFU count. Data are representative of at least two independent experiments or a compilation of four independent experiments (G and H). The results are expressed as the mean ± SEM (n = 4–6 mice per group). *, $P \leq 0.05$; **, $P \leq 0.01$; ***, $P \leq 0.001$.

order Clostridiales (phylum Firmicutes) was increased in STZ-injected WT mice. Overall, these results suggest that during STZ-induced diabetes, there is an alteration of the microbial composition in the gut, which may induce the bacterial translocation to the MLNs and PLNs. Additionally, antibiotic treatment was able to prevent the dysbiosis observed in STZ-injected WT mice, possibly contributing to the inability of bacteria to reach the PLNs in these mice.

Published June 20, 2016

NOD2 activation is sufficient to reestablish diabetes in diabetes-resistant, Abx-treated, STZ-injected WT mice

Because we found that antibiotic treatment abrogated the bacterial translocation to the PLNs (Fig. 6 D), possibly impairing NOD2 activation and the consequent induction of a pathogenic Th1 and Th17 cell immune response, we then analyzed whether the administration of Abx had any effect on diabetes incidence.

Interestingly, Abx-treated STZ-injected WT mice were completely resistant to STZ-induced T1D (Fig. 6, G and H), which supports the idea that the accumulation of commensal bacteria inside the PLNs plays a critical role in diabetes development. Notably, when Abx-treated STZ-injected WT mice received the NOD2 ligand MDP in their drinking water, both hyperglycemia and diabetes incidence were reestablished (Fig. 6, G and H), along with a robust inflammatory infiltrate within the pancreatic islets (Fig. 6, I, top, and J). Additionally, a reduction in insulin staining inside the pancreatic islets (Fig. 6, I, middle, and K) and in insulin levels in the serum (Fig. 6 M), together with an increase in β cell death analyzed by TUNEL staining (Fig. 6, I, bottom, and L), was also observed in Abx-treated STZ-injected WT mice provided with MDP. Collectively, these data suggest that the gut microbiota plays a crucial role in mediating STZ-induced diabetes via the activation of the NOD2 receptor inside the PLNs.

NOD2-deficient mice have already been shown to harbor a different gut microbiota composition compared with C57BL/6 WT mice (Riddle and Porter, 2012), which was later associated with an increase in regulatory T cells in the lamina propria (LP regulatory cells; Amendola et al., 2014). To rule out the possibility that $NOD2^{-/-}$ mice are resistant to STZ-induced T1D as a result of tolerogenic microbiota, Abx-treated $NOD2^{-/-}$ mice were transplanted with the microbiota of WT mice and were then injected with five doses of STZ. Interestingly, $NOD2^{-/-}$ mice harboring the gut microbiota of WT mice (NOD2[WT]) were still resistant to STZ-induced diabetes, suggesting that the absence of the NOD2 receptor rather than a tolerogenic microbiota is impairing diabetes development in $NOD2^{-/-}$ mice (Fig. 6 N). We also analyzed the presence of bacteria inside the MLNs and PLNs of STZ-injected $NOD2^{-/-}$ mice to exclude the possibility that these mice are resistant to STZ-induced diabetes because there is no translocation of bacteria to the PLNs. Interestingly, STZ-injected $NOD2^{-/-}$ mice had bacteria inside their MLNs (Fig. 6 O) and PLNs (Fig. 6 P) 15 d after the STZ injections. Surprisingly, bacteria were also found at earlier time points in $NOD2^{-/-}$ mice, such as 7 d after the STZ injections, and even in naive $NOD2^{-/-}$ mice. These data corroborate several studies that demonstrated the importance of the NOD2 receptor in maintaining homeostasis in the gut epithelial barrier (Philpott et al., 2014). Overall, these data suggest that resistance of $NOD2^{-/-}$ mice to STZ-induced diabetes is not a result of tolerogenic microbiota or impaired bacterial translocation to the PLNs.

MDP supplementation restores the generation of Th1 and Th17 cells in the PLNs after antibiotic treatment

To verify that the immune response triggered by the activation of the NOD2 receptor inside the PLNs is generated in situ and is not a recruitment of immune cells from the MLNs, several parameters were assessed in both MLNs and PLNs of STZ-injected and Abx-treated STZ-injected WT mice with or without MDP supplementation. Interestingly, no differences were found between groups inside the MLNs in total cell count (Fig. 7 A), number of $CD4^+$ (Fig. 7 B) or $CD8^+$ (Fig. 7 C) T cells, and number of Th1 (Fig. 7 D) or Th17 (Fig. 7 E) cells, or in tolerogenic $CD11b^+CD103^+$ DCs (Fig. 7 F). Alternatively, MDP administration restored both Th1 and Th17 cell populations in the PLNs (Fig. 7, G–K), suggesting that the polarization of these pathogenic T cells was confined to the local draining LNs. Collectively, these data suggest that the recognition of commensal microbiota-derived MDP by the NOD2 receptor plays a critical role in the generation of pathogenic Th1 and Th17 cells inside the PLNs during STZ-induced T1D pathogenesis.

We also analyzed the myeloid cell compartment in these groups to further evaluate its contribution in driving a pathogenic Th1 and Th17 cell immune response inside the PLNs. Interestingly, antibiotic treatment abrogated the recruitment of both macrophages (Fig. 7 L) and DCs (Fig. 7 M) to the PLNs after the STZ injections. Notably, MDP was able to partially restore the macrophage levels inside the PLNs (Fig. 7 L). When analyzing the function of these macrophages that are recruited to the PLNs after MDP administration, we observed that whereas macrophages from Abx-treated STZ-injected WT mice fail to induce the production of IL-6 (Fig. 7 N) and IL-12 (Fig. 7 O), MDP administration was able to partially restore this proinflammatory immune response, thus demonstrating the importance of the NOD2 receptor in promoting a proinflammatory microenvironment inside the PLNs with a consequent induction of a pathogenic Th1 and Th17 cell immune response. Surprisingly, the administration of the NOD2 ligand MDP without the STZ injections was also able to induce the production of IL-6 and IL-12 by macrophages (Fig. 7, N and O, respectively). However, these mice did not develop diabetes (unpublished data). These data suggest that the NOD2 activation by the gut microbiota and the release of autoantigens by the damaged β cells caused by the low doses of STZ act synergistically to promote a pathogenic immune response, thus leading to STZ-induced diabetes.

DISCUSSION

We show here the importance of NOD2 in driving a proinflammatory immune response by myeloid cells, inducing the differentiation of pathogenic Th1 and Th17 cells, thus resulting in pancreatic insulitis and the consequent destruction of insulin-producing pancreatic β cells and STZ-induced T1D development. Mice lacking NOD2, but not NOD1, did not develop STZ-induced T1D and were unable to induce a Th1 and Th17 immune response in the PLNs and pancreas. Fur-

Published June 20, 2016

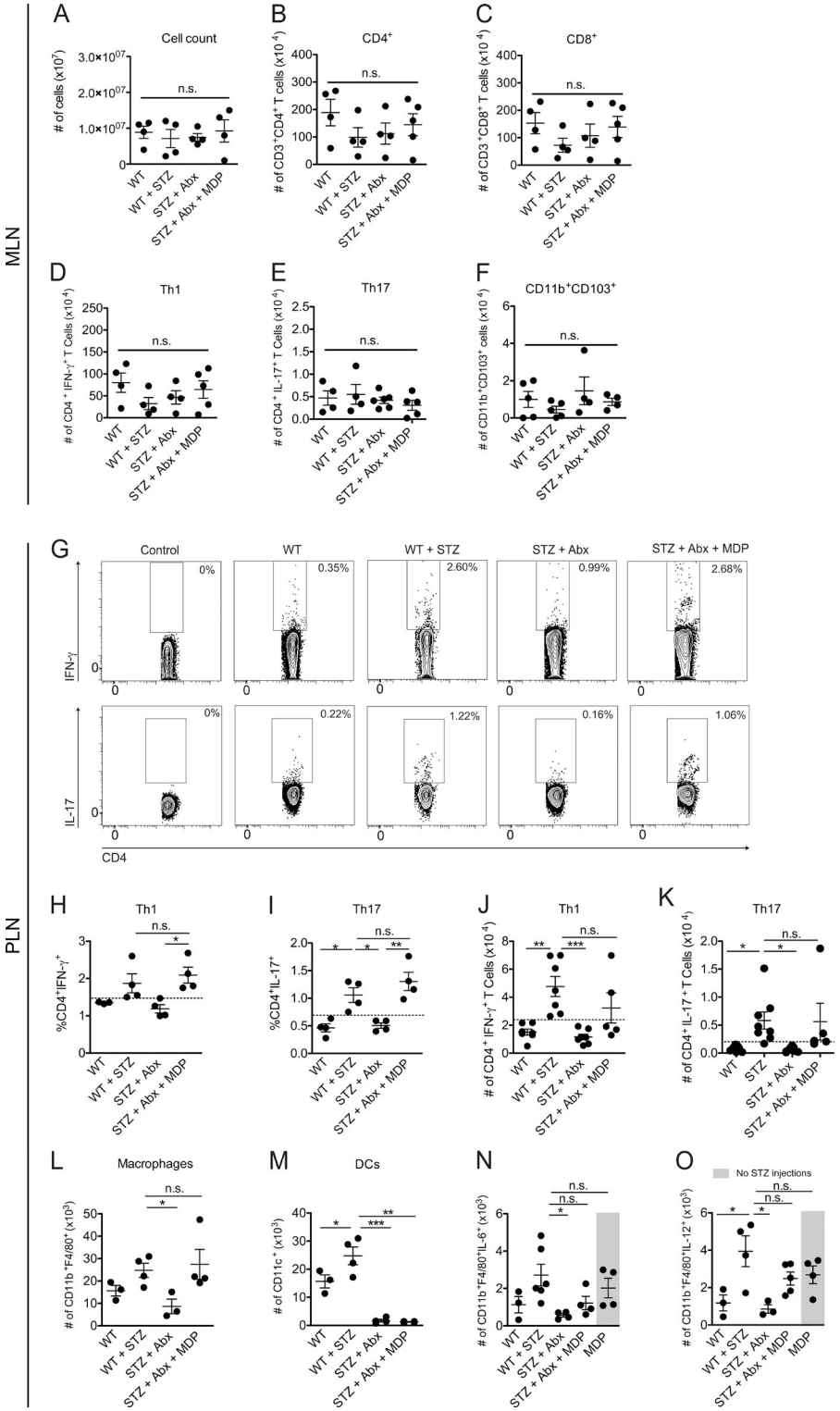

Figure 7. **NOD2 activation is sufficient to restore Th1 and Th17 cells in the PLNs of diabetes-resistant Abx-treated STZ-injected WT mice.** Cells from the MLNs or PLNs of STZ-injected WT mice that were treated with a cocktail of Abx and supplemented or not supplemented with MDP were recovered and analyzed for total number of cells (A) and absolute numbers of $CD4^+$ (B), $CD8^+$ (C), Th1 (D), Th17 (E), and tolerogenic $CD11b^+CD103^+$ DCs (F) in the MLNs, or the frequency (G–I) and absolute numbers (J and K) of Th1 and Th17 cells inside the PLNs by flow cytometry. The total numbers of macrophages (L) and DCs (M) of Abx-treated STZ-injected WT mice supplemented or not supplemented with MDP were analyzed by flow cytometry. The production of IL-6 (N) and IL-12 (O) by macrophages in the PLNs of WT mice that were treated with MDP but did not receive any STZ injections, or Abx-treated, STZ-injected WT mice supplemented or not supplemented with MDP, was analyzed by flow cytometry. The results are expressed as the mean ± SEM (n = 4–6 mice per group). *, $P \leq 0.05$; **, $P \leq 0.01$; ***, $P \leq 0.001$; n.s. = not significant.

thermore, diabetic mice had changes in the composition of the gut microbiota, which may be related to the observed bacterial translocation to the PLNs. Notably, antibiotic treatment impaired both the bacterial translocation to the PLNs and the changes in the gut microbiota, which was correlated with protection from the disease. Additionally, we show here that NOD2 plays a critical role in gut microbiota recognition because the addition of the NOD2 ligand, MDP, was sufficient to promote STZ-induced T1D in Abx-treated, STZ-injected WT mice. Interestingly, STZ-injected WT mice had

Published June 20, 2016

an increase in different clades of bacteria in the gut microbiota that have been associated with increased susceptibility to T1D in humans, which could contribute to the development of the disease. Thus, our results demonstrate a novel role for NOD2 in the development of STZ-induced T1D, providing a new clue to the possible mechanisms involved in gut microbiota recognition and T1D development.

In the present study, we show that the NOD2 receptor, which is responsible for recognizing bacteria-derived MDP, is crucial for triggering STZ-induced T1D. This occurs through the recognition of the gut microbiota by NOD2 and a consequent increase in IL-6– and IL-12–producing DCs and macrophages, as well as IL-17– and IFN-γ–producing $CD4^+$ and $CD8^+$ effector T cells in the PLNs. Of note, no differences between T cells and tolerogenic $CD11b^+CD103^+$ DCs were found in the MLNs, indicating that the differentiation of a pathogenic immune response is confined to the PLNs. Interestingly, our results show that this recognition by NOD2 does not activate the adaptor molecule Rip2 because STZ-injected $Rip2^{-/-}$ mice were able to induce the generation of Th1 and Th17 cells in the PLNs and developed STZ-induced T1D equivalently to WT mice. It has been shown by in vitro experiments that $Rip2^{-/-}$ cells stimulated with MDP still activate JNK1/2 and p38 MAP kinases, suggesting that NOD2-mediated MAP kinase activation may involve other CARD domain-containing adapter proteins (Yang et al., 2007). One possibility could be CARD9, as Card9-deficient mice exhibit defects in p38 MAP kinase and JNK activation in MDP-stimulated cells, whereas NF-κb activation remains unaffected (Hsu et al., 2007). Additionally, NOD2 has been shown to interact with CARD9 and activate both p38 and JNK1/2 MAP kinases (Parkhouse et al., 2014). Moreover, it has been shown that NOD2 is able to interact with other adaptor proteins, such as mitochondrial antiviral signaling (MAVS), during a viral infection (Sabbah et al., 2009). Therefore, we believe that NOD2 activation in our model may involve another adaptor protein instead of Rip2.

The fact that not only Th1 cells but also Th17 cells were down-regulated in diabetes-resistant $NOD2^{-/-}$ mice was also intriguing, considering that the role of Th17 cells in T1D is quite controversial. Although some studies show that IL-17 silencing does not protect NOD mice from T1D development (Joseph et al., 2012), results from other groups suggest a different outcome. The blockade of Th17 cells with a monoclonal anti–IL-17 antibody in the effector phase of the disease (10 wk of age) was shown to prevent NOD mice from developing diabetes (Emamaullee et al., 2009). Additionally, an increase in IL-17 was found in PBMCs from diabetic patients (Arif et al., 2011). In the MLD-STZ mouse model, our group has already shown that STZ-injected $IL\text{-}17R^{-/-}$ mice are resistant to STZ-induced T1D (Yaochite et al., 2013). Accordingly, IL-23 co-administered with subdiabetogenic doses of STZ led to diabetes development (Mensah-Brown et al., 2006), thus corroborating a pathogenic role of Th17 cells in the disease. Our results demonstrate that IL-17–producing $CD4^+$ and $CD8^+$ T cells were decreased in the PLNs of diabetes-resistant $NOD2^{-/-}$ mice, suggesting a pathogenic role for these cell subtypes in the disease. In addition, the presence of the NOD2 receptor in DCs was important in driving this Th17 immune response through the recognition of MDP and further production of cytokines important to the differentiation of Th17 cells, such as IL-1β, IL-6, and IL-23. Moreover, DCs from $NOD2^{-/-}$ mice produced lower levels of IL-12 in vitro and in vivo and were unable to induce the differentiation of Th1 cells in vitro, which was correlated with the reduction in IFN-γ–producing $CD4^+$ and $CD8^+$ T cells in vivo. Interestingly, T reg cells, M2 macrophages, and tolerogenic $CD11c^+CD11b^+$ DCs were also up-regulated in the PLNs of diabetes-resistant $NOD2^{-/-}$ mice. Overall, we believe that the activation of the NOD2 receptor in DCs plays an important role in this shift toward a proinflammatory microenvironment in the PLNs, inducing Th1 and Th17 cells and contributing to STZ-induced T1D susceptibility.

There is increasing evidence that environmental factors acting at the intestinal level, especially the diverse bacterial species that constitute the gut microbiota, are able to influence the course of autoimmune diseases in tissues outside the intestine both in humans and in preclinical models (Sorini and Falcone, 2013). However, whether this process occurs through the homing of effector T cells primed with microbiota antigen-loaded DCs from the intestines to other tissues or if the bacterial content from the gut microbiota itself is able to escape to other tissues and further activate autoreactive T cells remains poorly understood. The fact that NOD2 recognizes the bacterial component MDP and that NOD2 was up-regulated in the PLNs of STZ-injected WT mice and NOD mice led to the hypothesis that commensal bacteria from the gut are able to translocate to the PLNs, thus triggering NOD2 activation and contributing to the generation of pathogenic effector T cells. In fact, we observed bacterial translocation to the MLNs in STZ-injected WT mice and, interestingly, to the PLNs in both STZ and NOD mouse models. Moreover, when mice were treated with Abx before STZ injections, they were completely protected from STZ-induced T1D development; this was correlated with the absence of bacteria inside the PLNs, but not in the MLNs, and with the consequent reduction in the Th1 and Th17 cell populations inside the PLNs. Interestingly, when the NOD2 ligand MDP was added to the drinking water of mice treated with Abx, hyperglycemia was reestablished after the STZ injections. These mice had an increase in IL-6– and IL-12–producing myeloid cells and, consequently, in Th1 and Th17 cells in the PLNs but not in the MLNs, and a robust insulitis within the pancreatic tissue, thus confirming the role of NOD2 in recognizing these bacteria reaching the PLNs. Interestingly, we observed that the administration of MDP without the STZ injections is also able to induce production of proinflammatory cytokines by myeloid cells. However, these mice do not develop diabetes (unpublished data). Considering that STZ injections alone are not sufficient to trigger STZ-induced diabetes in Abx-treated WT mice and that MDP alone (with-

out STZ injections) was also not able to induce the disease, we strongly believe that both NOD2 activation and the release of autoantigens by the damaged β cells caused by the low doses of STZ injections act synergistically to reach a threshold of β cell death that leads to hyperglycemia and consequently to diabetes. When DCs capture autoantigens from the pancreatic tissue that are released by the β cell death after the STZ injections and present them in a proinflammatory microenvironment in the PLNs (caused by bacteria activating NOD2), they skew the response toward a proinflammatory Th1/Th17 cell phenotype. Likewise, when DCs capture these autoantigens induced by the STZ injections and present them inside a non-inflamed PLN (in the absence of NOD2 activation), these DCs will skew the response toward an antiinflammatory response through the induction of IL-10 and regulatory T cells.

Next, we assessed whether a different composition of the gut microbiota could also be associated with STZ-induced T1D development. Metagenomic analysis revealed that STZ-injected diabetic WT mice have an altered gut microbiota compared with vehicle-injected WT mice, with an increase in several genera of bacteria. Diabetic mice displayed a significant increase in the Bacteroidaceae family and the *Bacteroides* genus. These results recapitulate what has been found in type 1 diabetic patients, in which the Bacteroidetes phylum, the Bacteroidaceae family, and the *Bacteroides* genus were found to be more common in autoantibody-positive children than in autoantibody-negative peers (de Goffau et al., 2013). We also found differences in the *Bifidobacterium* genus. More specifically, we found that it was increased only in diabetic STZ-injected WT mice but not in diabetes-resistant, Abx-treated STZ-injected or vehicle-injected WT mice. Similar results were also found among type 1 diabetic patients (de Goffau et al., 2013; Murri et al., 2013).

Interestingly, diabetes-resistant Abx-treated STZ-injected WT mice displayed a gut microbiota similar to vehicle-injected WT mice. One major difference was the increase in the phylum Verrucomicrobia and, at the genus level, the increase in *Akkermansia* in these mice. It has been shown that the resistance to T1D development in NOD mice fed a gluten-free diet is associated with an increase in *Akkermansia* (Marietta et al., 2013). Additionally, mice fed polyphenol-rich cranberry extract were protected from diet-induced obesity, insulin resistance, and intestinal inflammation in the gut microbiota. Interestingly, this protection was also associated with an increase in *Akkermansia* (Anhê et al., 2015).

Another interesting finding was that *Oscillospira* was increased only in STZ-injected diabetic mice. It has been reported that *Oscillospira* may be an important gut microbe that mediates the disruption of the intestinal epithelial barrier, thus causing the translocation of bacteria from the gut in a high-fat diet-induced gut dysfunction (Lam et al., 2012). In this study, a negative correlation was found between the abundance of *Oscillospira* and molecules that are important in maintaining the integrity of the gut epithelial barrier, such as ZO-1. Therefore, these bacteria could be responsible for the so-called leaky gut phenomenon that has been extensively documented by the scientific community (Vaarala et al., 2008; Cani et al., 2009; Lee et al., 2010; Brown et al., 2011; van Belle et al., 2011). Considering that the peritoneal cavity is a route for microbes that escape from the gut microbiota (Emani et al., 2015) and that the PLNs are constantly sampling antigens that come from the peritoneum and the gut (Turley et al., 2005), we strongly believe that during STZ-induced diabetes, the bacteria or their microbial byproducts translocating from the gut microbiota are reaching the PLNs and promoting a proinflammatory microenvironment through the activation of the NOD2 receptor.

In summary, our results demonstrate that the gut microbiota recognition by NOD2 inside the PLNs is crucial in driving a Th1 and Th17 cell pathogenic immune response, thus contributing to STZ-induced T1D pathogenesis. These data suggest that the dysbiosis observed in type 1 diabetic patients might act as an important environmental trigger in the development of the disease and that strategies aiming at blocking NOD2 signaling early in the disease emerge as potential therapies to be applied in the future.

MATERIALS AND METHODS

Mice. 8–12-wk-old male NOD1$^{-/-}$, NOD2$^{-/-}$, and Rip2$^{-/-}$ mice generated on a C57BL/6 background were used, and the littermates of the corresponding knockout strains were used as controls. NOD/LtJ and NOR/LtJ mice were obtained from The Jackson Laboratory. Mice were reared under specific pathogen–free conditions. All animal procedures were approved by our local ethics committee (Comitê de Ética em Experimentação Animal [CETEA] from the University of São Paulo; Process number 193/2011).

Diabetes model. C57BL/6 mice ranging from 8 to 12 wk of age were daily injected i.p. with 40 mg/kg STZ (Sigma-Aldrich) for five consecutive days. STZ was diluted in sodium citrate buffer, pH 4.5, and immediately injected after preparation. Blood samples were collected from the tail vein of non-fasted mice, and glucose levels were determined with the glucometer system Accu-Chek Go (Roche). Mice were considered diabetic when glycemia was >200 mg/dl after two consecutive determinations. Control mice received only sodium citrate buffer (vehicle) i.p. for five consecutive days.

GTT and ITT. Mice were fasted for 12 h (GTT) or 6 h (ITT). Next, a solution of 25% glucose (2 g/kg body weight) for the GTT or a solution of insulin (1.5 µI/kg body weight) for the ITT was administered into the peritoneal cavity. Blood samples were collected from the tail vein at 0, 5, 10, 15, 20, 25, and 30 min for the determination of blood glucose levels.

Bone marrow–derived macrophages and DCs. Bone marrow–derived macrophages from WT or NOD2$^{-/-}$ mice were ob-

Published June 20, 2016

tained as previously described (Silva et al., 2013). The macrophages were then stimulated with IFN-γ (200 ng/ml) and LPS (1 μg/ml) for 48 h in the presence or absence of MDP (10 μg/ml). The supernatant was collected for cytokine quantification. Alternatively, bone marrow–derived DCs from either WT or NOD2$^{-/-}$ mice were obtained as previously described (Carregaro et al., 2008). Cells were then stimulated with LPS (200 ng/ml) for 24 h in the presence or absence of MDP (10 μg/ml). The supernatant was collected for cytokine quantification.

Antibodies and flow cytometry. The following monoclonal antibody conjugates were used: CD3ε (145-2C11), APC-Cy7; CD4 (RM4-5), PerCP; CD8α (53–6.7), FITC; IL-17 (TC11-18H10), Alexa Fluor 647 and PE; IFN-γ (557998), Alexa Fluor 700; RORγt (AFKJS), PE; Foxp3 (MF23), Alexa Fluor 647; CD11b (M1/70), Pe-Cy7; CD11c (HL3), APC-Cy7; F4/80 (BM8), PerCP-Cy5; IL-10 (JES5-16E3), APC and CD206 (C068C2), APC. All antibodies were obtained from BD or eBioscience. FACSCanto II or AccuriC6 (both from BD) cytometers were used for flow cytometry, and the data were analyzed using FlowJo (Tree Star). Fluorescence-activated cell sorting was performed using a FACSAria flow cytometer (BD). The isolation of naive CD4$^+$ T cells for the in vitro experiments was performed with the CD4$^+$ T Cell Isolation kit (Miltenyi Biotec). For the intracellular staining, cells were stimulated for 4 h with 50 ng/ml PMA (Sigma-Aldrich), 500 ng/ml ionomycin (Sigma-Aldrich), and Golgi Stop (1,000 X; BD). Cells were fixed in PBS containing 4% paraformaldehyde and permeabilized in PBS containing 1% FBS, 0.1% sodium azide, and 0.2% saponin. Antibodies were then added and cells were incubated for 20 min at 4°C. After the staining, the cells were washed and fixed in PBS containing 1% paraformaldehyde and further analyzed in a FACSCanto II or BD Accuri C6 cytometer.

Antibiotic treatment, MDP supplementation, and fecal transplantation. Mice were administered daily doses of 1.86 mg ampicillin (Sigma-Aldrich), 0.96 mg vancomycin (Sigma-Aldrich), 1.86 mg neomycin sulfate (Sigma-Aldrich), and 1.86 mg metronidazole (Sigma-Aldrich) diluted in 300 μl of drinking water by gavage for 2 wk before the injections with STZ. Throughout Abx administration, mice were supplemented or not supplemented with MDP (Sigma-Aldrich) in the drinking water at a fixed concentration of 1 μM to reconstitute MDP in the intestine. Alternatively, NOD2$^{-/-}$ mice were treated with Abx for 2 wk, and then gavaged with 200 μl of fecal samples from C57BL/6 WT mice diluted in PBS. 10 d later, after their gut microbiota were colonized by the WT microbiota, these NOD2$^{-/-}$ (designated as (NOD2[WT]) mice were injected with five doses of STZ and were analyzed for blood glucose levels 15 d later.

Histology and immunohistochemistry. Pancreatic tissue was fixed in 10% formalin and embedded in paraffin. 5-μm sections were affixed to slides, deparaffinized, and stained with hematoxylin and eosin (H&E). Morphological changes in the stained sections were examined under a light microscope. Immunohistochemistry reactions were performed on sections (5 μm) of formalin-fixed tissue, as previously described (Yaochite et al., 2013). In brief, the sections were dewaxed, rehydrated, and incubated with peroxidase-blocking reagent (Dako) to block endogenous peroxidase. Next, the slides were incubated with PBS plus BSA 1% to block unspecific binding. Next, rabbit monoclonal anti–mouse insulin antibodies (Santa Cruz Biotechnology, Inc.) were applied to the sections, followed by incubation with LSABTM$^+$ kit/HRP (Dako). The slides were stained with diaminobenzidine (DAB) according to the manufacturer's instructions (Dako). Finally, the sections were counterstained with hematoxylin, mounted, and analyzed. Alternatively, the In Situ Cell Death Detection kit (Roche) was used for the TUNEL staining, according to the manufacturer's instructions. For the insulitis score, ∼100 islets per group were analyzed and classified as no insulitis, peri-insulitis, and invasive insulitis.

Serum insulin quantification. The insulin concentration in the serum was determined using the Mouse Ultrasensitive Insulin ELISA kit (Alpco Diagnostics) according to the manufacturer's instructions.

Cytokine quantification. Pancreatic tissue was homogenized and centrifuged at 500 *g* for 10 min, and the supernatant was collected for the assessment of mouse IL-10, IL-17, and IFN-γ production (BD or R&D Systems) according to the manufacturer's instructions. Similarly, the supernatant from in vitro experiments was collected and analyzed for IL-1β, IL-6, IL-12p40, IL-17, IL-23, or IFN-γ production (BD or R&D Systems) according to the manufacturer's instructions.

Real-time PCR. Real-time PCR was performed as previously described (Spiller et al., 2012). In brief, mice were sacrificed, and the PLNs were collected. Total RNA was extracted with TRIzol reagent (Invitrogen) after the manufacturer's instructions. Reverse transcription of total RNA to cDNA was performed with a reverse transcription reaction kit (Superscript II; Gibco). Quantitative mRNA analysis by real-time PCR was performed with a StepOnePlus Real-Time PCR System (Life Technologies) using the SYBR Green fluorescence system as indicated by the manufacturer.

16S rRNA gene sequencing and statistical analyses. 16S rRNA gene sequencing was performed as previously described (Palm et al., 2014). The Ribosomal Database Project classifier (RDP) and the May 2013 Greengenes taxonomy were used to assign taxonomy to representative OTUs (Lozupone and Knight, 2005; Wang et al., 2007; Caporaso et al., 2010), and the Linear Discriminant Analysis Effect Size Galaxy module was used for additional statistical analyses (Segata et al., 2011).

DNA extraction and 16S rRNA gene PCR analysis. The DNA extraction from the pancreatic LNs was performed using a DNeasy Blood and Tissue kit (QIAGEN) following the manufacturer's instructions. For the PCR analysis, 10 ng of DNA and 5 µM of the 16S primer (forward, 5′-TGGCTCAGGACG AACGCTGGCGGC-3′; reverse, 5′-CCTACTGCTGCC TCCCGTAGGAGT-3′) were used. The amplifications were performed in a QuantStudio 12K Flex (Applied Biosystems).

Statistical analysis. The results were expressed as the mean ± SEM. Differences between two unpaired groups were compared by Student's *t* test. Statistical variations between three or more groups within an experiment were analyzed by one-way ANOVA, followed by Tukey's post-test, using the Prism 6.0 statistical program (GraphPad). $P < 0.05$ was considered statistically significant.

ACKNOWLEDGMENTS

We would like to thank Elaine Medeiros Floriano (Ribeirão Preto Medical School, University of São Paulo [FMRP-USP], São Paulo, Brazil), for the assistance with the tissue processing for the histopathological analysis. We also thank Juliana N.U. Yaochite, Rodrigo P.A. Rodrigues, and Maria do Carmo Souza from the Department of Biochemistry and Immunology (FMRP-USP) for the assistance with the PLNs processing and CFU counting.

This research received funding from the São Paulo Research Foundation under grant agreement nos. 2012/10395-0 (Project Young Researcher) and 2013/08216-2 (Center for Research in Inflammatory Disease) and from the University of São Paulo (Núcleo de Pesquisa em Doenças Inflamatórias) under grant agreement no. 11.1.21625.01.0.

The authors declare no competing financial interests.

Submitted: 29 April 2015
Accepted: 5 May 2016

REFERENCES

Amendola, A., A. Butera, M. Sanchez, W. Strober, and M. Boirivant. 2014. Nod2 deficiency is associated with an increased mucosal immunoregulatory response to commensal microorganisms. *Mucosal Immunol.* 7:391–404. http://dx.doi.org/10.1038/mi.2013.58

Anhê, F.F., D. Roy, G. Pilon, S. Dudonné, S. Matamoros, T.V. Varin, C. Garofalo, Q. Moine, Y. Desjardins, E. Levy, and A. Marette. 2015. A polyphenol-rich cranberry extract protects from diet-induced obesity, insulin resistance and intestinal inflammation in association with increased *Akkermansia* spp. population in the gut microbiota of mice. *Gut.* 64:872–883. http://dx.doi.org/10.1136/gutjnl-2014-307142

Arata, M., L. Bruno, C. Pastorale, F. Pagliero, and J.C. Basabe. 2001. Effect of modified diabetic splenocytes on mice injected with splenocytes from multiple low-dose streptozotocin diabetic donors. *Exp. Biol. Med. (Maywood).* 226:898–905.

Arif, S., F. Moore, K. Marks, T. Bouckenooghe, C.M. Dayan, R. Planas, M. Vives-Pi, J. Powrie, T. Tree, P. Marchetti, et al. 2011. Peripheral and islet interleukin-17 pathway activation characterizes human autoimmune diabetes and promotes cytokine-mediated β-cell death. *Diabetes.* 60:2112–2119. http://dx.doi.org/10.2337/db10-1643

Bach, J.-F. 2002. The effect of infections on susceptibility to autoimmune and allergic diseases. *N. Engl. J. Med.* 347:911–920. http://dx.doi.org/10.1056/NEJMra020100

Benjamin, J.L., R. Sumpter Jr., B. Levine, and L.V. Hooper. 2013. Intestinal epithelial autophagy is essential for host defense against invasive bacteria. *Cell Host Microbe.* 13:723–734. http://dx.doi.org/10.1016/j.chom.2013.05.004

Bollyky, P.L., J.B. Bice, I.R. Sweet, B.A. Falk, J.A. Gebe, A.E. Clark, V.H. Gersuk, A. Aderem, T.R. Hawn, and G.T. Nepom. 2009. The toll-like receptor signaling molecule Myd88 contributes to pancreatic beta-cell homeostasis in response to injury. *PLoS One.* 4:e5063. http://dx.doi.org/10.1371/journal.pone.0005063

Bosi, E., L. Molteni, M.G. Radaelli, L. Folini, I. Fermo, E. Bazzigaluppi, L. Piemonti, M.R. Pastore, and R. Paroni. 2006. Increased intestinal permeability precedes clinical onset of type 1 diabetes. *Diabetologia.* 49:2824–2827. http://dx.doi.org/10.1007/s00125-006-0465-3

Brown, C.T., A.G. Davis-Richardson, A. Giongo, K.A. Gano, D.B. Crabb, N. Mukherjee, G. Casella, J.C. Drew, J. Ilonen, M. Knip, et al. 2011. Gut microbiome metagenomics analysis suggests a functional model for the development of autoimmunity for type 1 diabetes. *PLoS One.* 6:e25792. http://dx.doi.org/10.1371/journal.pone.0025792

Brugman, S., F.A. Klatter, J.T.J. Visser, A.C.M. Wildeboer-Veloo, H.J.M. Harmsen, J. Rozing, and N.A. Bos. 2006. Antibiotic treatment partially protects against type 1 diabetes in the Bio-Breeding diabetes-prone rat. Is the gut flora involved in the development of type 1 diabetes? *Diabetologia.* 49:2105–2108. http://dx.doi.org/10.1007/s00125-006-0334-0

Caetano, B.C., A. Biswas, D.S. Lima Jr., L. Benevides, T.W.P. Mineo, C.V. Horta, K.-H. Lee, J.S. Silva, R.T. Gazzinelli, D.S. Zamboni, and K.S. Kobayashi. 2011. Intrinsic expression of Nod2 in $CD4^+$ T lymphocytes is not necessary for the development of cell-mediated immunity and host resistance to *Toxoplasma gondii*. *Eur. J. Immunol.* 41:3627–3631. http://dx.doi.org/10.1002/eji.201141876

Cani, P.D., S. Possemiers, T. Van de Wiele, Y. Guiot, A. Everard, O. Rottier, L. Geurts, D. Naslain, A. Neyrinck, D.M. Lambert, et al. 2009. Changes in gut microbiota control inflammation in obese mice through a mechanism involving GLP-2-driven improvement of gut permeability. *Gut.* 58:1091–1103. http://dx.doi.org/10.1136/gut.2008.165886

Caporaso, J.G., J. Kuczynski, J. Stombaugh, K. Bittinger, F.D. Bushman, E.K. Costello, N. Fierer, A.G. Peña, J.K. Goodrich, J.I. Gordon, et al.. 2010. QIIME allows analysis of high-throughput community sequencing data Intensity normalization improves color calling in SOLiD sequencing. *Nat. Publ. Gr.* 7:335–336. http://dx.doi.org/10.1038/nmeth0510-335

Carregaro, V., J.G. Valenzuela, T.M. Cunha, W.A. Verri Jr., R. Grespan, G. Matsumura, J.M.C. Ribeiro, D.-E. Elnaiem, J.S. Silva, and F.Q. Cunha. 2008. Phlebotomine salivas inhibit immune inflammation-induced neutrophil migration via an autocrine DC-derived PGE2/IL-10 sequential pathway. *J. Leukoc. Biol.* 84:104–114. http://dx.doi.org/10.1189/jlb.1107797

Coppieters, K.T., T. Boettler, and M. von Herrath. 2012. Virus infections in type 1 diabetes. *Cold Spring Harb. Perspect. Med.* 2:a007682. http://dx.doi.org/10.1101/cshperspect.a007682

Craighead, J.E., and M.F. McLane. 1968. Diabetes mellitus: induction in mice by encephalomyocarditis virus. *Science.* 162:913–914. http://dx.doi.org/10.1126/science.162.3856.913

de Goffau, M.C., K. Luopajärvi, M. Knip, J. Ilonen, T. Ruohtula, T. Härkönen, L. Orivuori, S. Hakala, G.W. Welling, H.J. Harmsen, and O. Vaarala. 2013. Fecal microbiota composition differs between children with β-cell autoimmunity and those without. *Diabetes.* 62:1238–1244. http://dx.doi.org/10.2337/db12-0526

Devaraj, S., P. Tobias, and I. Jialal. 2011a. Corrigendum to "Knockout of toll-like receptor-4 attenuates the pro-inflammatory state of diabetes". *Cytokine.* 56:832. http://dx.doi.org/10.1016/j.cyto.2011.09.008

Devaraj, S., P. Tobias, B.S. Kasinath, R. Ramsamooj, A. Afify, and I. Jialal. 2011b. Knockout of toll-like receptor-2 attenuates both the proinflammatory state of diabetes and incipient diabetic nephropathy. *Arterioscler. Thromb.*

Vasc. Biol. 31:1796–1804. http://dx.doi.org/10.1161/ATVBAHA.111.228924

Dinh, D.M., G.E. Volpe, C. Duffalo, S. Bhalchandra, A.K. Tai, A.V. Kane, C.A. Wanke, and H.D. Ward. 2015. Intestinal microbiota, microbial translocation, and systemic inflammation in chronic HIV infection. *J. Infect. Dis.* 211:19–27. http://dx.doi.org/10.1093/infdis/jiu409

Earley, Z.M., S. Akhtar, S.J. Green, A. Naqib, O. Khan, A.R. Cannon, A.M. Hammer, N.L. Morris, X. Li, J.M. Eberhardt, et al. 2015. Burn injury alters the intestinal microbiome and increases gut permeability and bacterial translocation. *PLoS One.* 10:e0129996. http://dx.doi.org/10.1371/journal.pone.0129996

Elias, D., H. Prigozin, N. Polak, M. Rapoport, A.W. Lohse, and I.R. Cohen. 1994. Autoimmune diabetes induced by the beta-cell toxin STZ. Immunity to the 60-kDa heat shock protein and to insulin. *Diabetes.* 43:992–998. http://dx.doi.org/10.2337/diab.43.8.992

Emamaullee, J.A., J. Davis, S. Merani, C. Toso, J.F. Elliott, A. Thiesen, and A.M.J. Shapiro. 2009. Inhibition of Th17 cells regulates autoimmune diabetes in NOD mice. *Diabetes.* 58:1302–1311. http://dx.doi.org/10.2337/db08-1113

Emani, R., C. Alam, S. Pekkala, S. Zafar, M.R. Emani, and A. Hänninen. 2015. Peritoneal cavity is a route for gut-derived microbial signals to promote autoimmunity in non-obese diabetic mice. *Scand. J. Immunol.* 81:102–109. http://dx.doi.org/10.1111/sji.12253

Gillespie, K.M., S.C. Bain, A.H. Barnett, P.J. Bingley, M.R. Christie, G.V. Gill, and E.A. Gale. 2004. The rising incidence of childhood type 1 diabetes and reduced contribution of high-risk HLA haplotypes. *Lancet.* 364:1699–1700. http://dx.doi.org/10.1016/S0140-6736(04)17357-1

Gitelman, S.E., P.A. Gottlieb, M.R. Rigby, E.I. Felner, S.M. Willi, L.K. Fisher, A. Moran, M. Gottschalk, W.V. Moore, A. Pinckney, et al. START Study Team. 2013. Antithymocyte globulin treatment for patients with recent-onset type 1 diabetes: 12-month results of a randomised, placebo-controlled, phase 2 trial. *Lancet Diabetes Endocrinol.* 1:306–316. http://dx.doi.org/10.1016/S2213-8587(13)70065-2

Hsu, Y.-M.S., Y. Zhang, Y. You, D. Wang, H. Li, O. Duramad, X.-F. Qin, C. Dong, and X. Lin. 2007. The adaptor protein CARD9 is required for innate immune responses to intracellular pathogens. *Nat. Immunol.* 8:198–205. http://dx.doi.org/10.1038/ni1426

Joseph, J., S. Bittner, F.M.P. Kaiser, H. Wiendl, and S. Kissler. 2012. IL-17 silencing does not protect nonobese diabetic mice from autoimmune diabetes. *J. Immunol.* 188:216–221. http://dx.doi.org/10.4049/jimmunol.1101215

Kim, H.S., M.S. Han, K.W. Chung, S. Kim, E. Kim, M.J. Kim, E. Jang, H.A. Lee, J. Youn, S. Akira, and M.S. Lee. 2007. Toll-like receptor 2 senses beta-cell death and contributes to the initiation of autoimmune diabetes. *Immunity.* 27:321–333. http://dx.doi.org/10.1016/j.immuni.2007.06.010

Kriegel, M.A., C. Rathinam, and R.A. Flavell. 2012. Pancreatic islet expression of chemokine CCL2 suppresses autoimmune diabetes via tolerogenic $CD11c^+$ $CD11b^+$ dendritic cells. *Proc. Natl. Acad. Sci. USA.* 109:3457–3462. http://dx.doi.org/10.1073/pnas.1115308109

Krogvold, L., B. Edwin, T. Buanes, G. Frisk, O. Skog, M. Anagandula, O. Korsgren, D. Undlien, M.C. Eike, S.J. Richardson, et al. 2015. Detection of a low-grade enteroviral infection in the islets of langerhans of living patients newly diagnosed with type 1 diabetes. *Diabetes.* 64:1682–1687. http://dx.doi.org/10.2337/db14-1370

Lam, Y.Y., C.W.Y. Ha, C.R. Campbell, A.J. Mitchell, A. Dinudom, J. Oscarsson, D.I. Cook, N.H. Hunt, I.D. Caterson, A.J. Holmes, and L.H. Storlien. 2012. Increased gut permeability and microbiota change associate with mesenteric fat inflammation and metabolic dysfunction in diet-induced obese mice. *PLoS One.* 7:e34233. http://dx.doi.org/10.1371/journal.pone.0034233

Lee, A.S., D.L. Gibson, Y. Zhang, H.P. Sham, B.A. Vallance, and J.P. Dutz. 2010. Gut barrier disruption by an enteric bacterial pathogen accelerates insulitis in NOD mice. *Diabetologia.* 53:741–748. http://dx.doi.org/10.1007/s00125-009-1626-y

Leiter, E.H. 1982. Multiple low-dose streptozotocin-induced hyperglycemia and insulitis in C57BL mice: influence of inbred background, sex, and thymus. *Proc. Natl. Acad. Sci. USA.* 79:630–634. http://dx.doi.org/10.1073/pnas.79.2.630

Like, A.A., and A.A. Rossini. 1976. Streptozotocin-induced pancreatic insulitis: new model of diabetes mellitus. *Science.* 193:415–417. http://dx.doi.org/10.1126/science.180605

Lozupone, C., and R. Knight. 2005. UniFrac: a new phylogenetic method for comparing microbial communities. *Appl. Environ. Microbiol.* 71:8228–8235. http://dx.doi.org/10.1128/AEM.71.12.8228-8235.2005

Marietta, E.V., A.M. Gomez, C. Yeoman, A.Y. Tilahun, C.R. Clark, D.H. Luckey, J.A. Murray, B.A. White, Y.C. Kudva, and G. Rajagopalan. 2013. Low incidence of spontaneous type 1 diabetes in non-obese diabetic mice raised on gluten-free diets is associated with changes in the intestinal microbiome. *PLoS One.* 8:e78687. http://dx.doi.org/10.1371/journal.pone.0078687

Mensah-Brown, E.P.K., A. Shahin, M. Al-Shamisi, X. Wei, and M.L. Lukic. 2006. IL-23 leads to diabetes induction after subdiabetogenic treatment with multiple low doses of streptozotocin. *Eur. J. Immunol.* 36:216–223. http://dx.doi.org/10.1002/eji.200535325

Moran, A., B. Bundy, D.J. Becker, L.A. DiMeglio, S.E. Gitelman, R. Goland, C.J. Greenbaum, K.C. Herold, J.B. Marks, P. Raskin, et al. AIDA Study Group. 2013. Interleukin-1 antagonism in type 1 diabetes of recent onset: two multicentre, randomised, double-blind, placebo-controlled trials. *Lancet.* 381:1905–1915. http://dx.doi.org/10.1016/S0140-6736(13)60023-9

Murri, M., I. Leiva, J.M. Gomez-Zumaquero, F.J. Tinahones, F. Cardona, F. Soriguer, and M.I. Queipo-Ortuño. 2013. Gut microbiota in children with type 1 diabetes differs from that in healthy children: a case-control study. *BMC Med.* 11:46. http://dx.doi.org/10.1186/1741-7015-11-46

O'Brien, C.L., P. Pavli, D.M. Gordon, and G.E. Allison. 2014. Detection of bacterial DNA in lymph nodes of Crohn's disease patients using high throughput sequencing. *Gut.* 63:1596–1606. http://dx.doi.org/10.1136/gutjnl-2013-305320

Paik, S.G., N. Fleischer, and S.I. Shin. 1980. Insulin-dependent diabetes mellitus induced by subdiabetogenic doses of streptozotocin: obligatory role of cell-mediated autoimmune processes. *Proc. Natl. Acad. Sci. USA.* 77:6129–6133. http://dx.doi.org/10.1073/pnas.77.10.6129

Palm, N.W., M.R. de Zoete, T.W. Cullen, N.A. Barry, J. Stefanowski, L. Hao, P.H. Degnan, J. Hu, I. Peter, W. Zhang, et al. 2014. Immunoglobulin A coating identifies colitogenic bacteria in inflammatory bowel disease. *Cell.* 158:1000–1010. http://dx.doi.org/10.1016/j.cell.2014.08.006

Parkhouse, R., J.P. Boyle, S. Mayle, K. Sawmynaden, K. Rittinger, and T.P. Monie. 2014. Interaction between NOD2 and CARD9 involves the NOD2 NACHT and the linker region between the NOD2 CARDs and NACHT domain. *FEBS Lett.* 588:2830–2836. http://dx.doi.org/10.1016/j.febslet.2014.06.035

Philpott, D.J., M.T. Sorbara, S.J. Robertson, K. Croitoru, and S.E. Girardin. 2014. NOD proteins: regulators of inflammation in health and disease. *Nat. Rev. Immunol.* 14:9–23. http://dx.doi.org/10.1038/nri3565

Reed, J.C., and K.C. Herold. 2015. Thinking bedside at the bench: the NOD mouse model of T1DM. *Nat. Rev. Endocrinol.* 11:308–314. http://dx.doi.org/10.1038/nrendo.2014.236

Rees, D.A., and J.C. Alcolado. 2005. Animal models of diabetes mellitus. *Diabet. Med.* 22:359–370. http://dx.doi.org/10.1111/j.1464-5491.2005.01499.x

Riddle, M.S., and C.K. Porter. 2012. Detection bias and the association between inflammatory bowel disease and Salmonella and Campylobacter

infection. *Gut.* 61:635–635. http://dx.doi.org/10.1136/gutjnl-2011-300617

Sabbah, A., T.H. Chang, R. Harnack, V. Frohlich, K. Tominaga, P.H. Dube, Y. Xiang, and S. Bose. 2009. Activation of innate immune antiviral responses by Nod2. *Nat. Immunol.* 10:1073–1080. http://dx.doi.org/10.1038/ni.1782

Savilahti, E., T. Ormälä, T. Saukkonen, U. Sandini-Pohjavuori, J.M. Kantele, A. Arato, J. Ilonen, and H.K. Åkerblom. 1999. Jejuna of patients with insulin-dependent diabetes mellitus (IDDM) show signs of immune activation. *Clin. Exp. Immunol.* 116:70–77. http://dx.doi.org/10.1046/j.1365-2249.1999.00860.x

Secondulfo, M., D. Iafusco, R. Carratù, L. deMagistris, A. Sapone, M. Generoso, A. Mezzogiomo, F.C. Sasso, M. Cartenì, R. De Rosa, et al. 2004. Ultrastructural mucosal alterations and increased intestinal permeability in non-celiac, type I diabetic patients. *Dig. Liver Dis.* 36:35–45. http://dx.doi.org/10.1016/j.dld.2003.09.016

Segata, N., J. Izard, L. Waldron, D. Gevers, L. Miropolsky, W.S. Garrett, and C. Huttenhower. 2011. Metagenomic biomarker discovery and explanation. *Genome Biol.* 12:R60. http://dx.doi.org/10.1186/gb-2011-12-6-r60

Silva, G.K., R.S. Costa, T.N. Silveira, B.C. Caetano, C.V. Horta, F.R.S. Gutierrez, P.M.D. Guedes, W.A. Andrade, M. De Niz, R.T. Gazzinelli, et al. 2013. Apoptosis-associated speck-like protein containing a caspase recruitment domain inflammasomes mediate IL-1β response and host resistance to *Trypanosoma cruzi* infection. *J. Immunol.* 191:3373–3383. http://dx.doi.org/10.4049/jimmunol.1203293

Sorini, C., and M. Falcone. 2013. Shaping the (auto)immune response in the gut: the role of intestinal immune regulation in the prevention of type 1 diabetes. *Am. J. Clin. Exp. Immunol.* 2:156–171.

Spiller, F., D. Carlos, F.O. Souto, A. de Freitas, F.S. Soares, S.M. Vieira, F.J.A. Paula, J.C. Alves-Filho, and F.Q. Cunha. 2012. α1-Acid glycoprotein decreases neutrophil migration and increases susceptibility to sepsis in diabetic mice. *Diabetes.* 61:1584–1591. http://dx.doi.org/10.2337/db11-0825

Tada, H., S. Aiba, K. Shibata, T. Ohteki, and H. Takada. 2005. Synergistic effect of Nod1 and Nod2 agonists with toll-like receptor agonists on human dendritic cells to generate interleukin-12 and T helper type 1 cells. *Infect. Immun.* 73:7967–7976. http://dx.doi.org/10.1128/IAI.73.12.7967-7976.2005

Tiittanen, M., M. Westerholm-Ormio, M. Verkasalo, E. Savilahti, and O. Vaarala. 2008. Infiltration of forkhead box P3-expressing cells in small intestinal mucosa in coeliac disease but not in type 1 diabetes. *Clin. Exp. Immunol.* 152:498–507. http://dx.doi.org/10.1111/j.1365-2249.2008.03662.x

Tsuji, Y., T. Watanabe, M. Kudo, H. Arai, W. Strober, and T. Chiba. 2012. Sensing of commensal organisms by the intracellular sensor NOD1 mediates experimental pancreatitis. *Immunity.* 37:326–338. http://dx.doi.org/10.1016/j.immuni.2012.05.024

Turley, S.J., J.-W. Lee, N. Dutton-Swain, D. Mathis, and C. Benoist. 2005. Endocrine self and gut non-self intersect in the pancreatic lymph nodes. *Proc. Natl. Acad. Sci. USA.* 102:17729–17733. http://dx.doi.org/10.1073/pnas.0509006102

Vaarala, O., M.A. Atkinson, and J. Neu. 2008. The "perfect storm" for type 1 diabetes: the complex interplay between intestinal microbiota, gut permeability, and mucosal immunity. *Diabetes.* 57:2555–2562. http://dx.doi.org/10.2337/db08-0331

Valle, A., G.M. Giamporcaro, M. Scavini, A. Stabilini, P. Grogan, E. Bianconi, G. Sebastiani, M. Masini, N. Maugeri, L. Porretti, et al. 2013. Reduction of circulating neutrophils precedes and accompanies type 1 diabetes. *Diabetes.* 62:2072–2077. http://dx.doi.org/10.2337/db12-1345

van Belle, T.L., K.T. Coppieters, and M.G. von Herrath. 2011. Type 1 diabetes: etiology, immunology, and therapeutic strategies. *Physiol. Rev.* 91:79–118. http://dx.doi.org/10.1152/physrev.00003.2010

von Herrath, M.G., J. Dockter, and M.B. Oldstone. 1994. How virus induces a rapid or slow onset insulin-dependent diabetes mellitus in a transgenic model. *Immunity.* 1:231–242. http://dx.doi.org/10.1016/1074-7613(94)90101-5

Wang, Q., G.M. Garrity, J.M. Tiedje, and J.R. Cole. 2007. Naive Bayesian classifier for rapid assignment of rRNA sequences into the new bacterial taxonomy. *Appl. Environ. Microbiol.* 73:5261–5267. http://dx.doi.org/10.1128/AEM.00062-07

Westerholm-Ormio, M., O. Vaarala, P. Pihkala, J. Ilonen, and E. Savilahti. 2003. Immunologic activity in the small intestinal mucosa of pediatric patients with type 1 diabetes. *Diabetes.* 52:2287–2295. http://dx.doi.org/10.2337/diabetes.52.9.2287

Yang, Y., C. Yin, A. Pandey, D. Abbott, C. Sassetti, and M.A. Kelliher. 2007. NOD2 pathway activation by MDP or Mycobacterium tuberculosis infection involves the stable polyubiquitination of Rip2. *J. Biol. Chem.* 282:36223–36229. http://dx.doi.org/10.1074/jbc.M703079200

Yaochite, J.N., C. Caliari-Oliveira, M.R. Davanso, D. Carlos, K.C. Malmegrim, C.R. Cardoso, L.N. Ramalho, P.V. Palma, J.S. da Silva, F.Q. Cunha, et al. 2013. Dynamic changes of the Th17/Tc17 and regulatory T cell populations interfere in the experimental autoimmune diabetes pathogenesis. *Immunobiology.* 218:338–352. http://dx.doi.org/10.1016/j.imbio.2012.05.010

Ylipaasto, P., T. Smura, P. Gopalacharyulu, A. Paananen, T. Seppänen-Laakso, S. Kaijalainen, H. Ahlfors, O. Korsgren, J.R. Lakey, R. Lahesmaa, et al. 2012. Enterovirus-induced gene expression profile is critical for human pancreatic islet destruction. *Diabetologia.* 55:3273–3283. http://dx.doi.org/10.1007/s00125-012-2713-z

Yoon, J.W., M. Austin, T. Onodera, and A.L. Notkins. 1979. Isolation of a virus from the pancreas of a child with diabetic ketoacidosis. *N. Engl. J. Med.* 300:1173–1179. http://dx.doi.org/10.1056/NEJM197905243002102